國立臺灣大學理學院物理學系

碩士論文

Department of Physics
College of Science
National Taiwan University

Master Thesis

非馬可夫開放系統中量子邏輯閘的最佳化控制

Optimal Control of Quantum Gates for a Non-Markovian Open Quantum Qubit System

黃 斌
Bin Hwang

指導教授：管希聖 博士
Advisor: Goan Hsi-Sheng, Ph.D.

中華民國 100 年 6 月
June, 2011

致謝

得以順利完成此篇碩士論文，首先要感謝我的指導教授管希聖博士，儘管教授有繁重的教學與工作要忙，老師依然很樂意與學生討論並指導研究學習上的難題。甚至在許多細節上也有著充分的耐心與態度，尤其在我做研究中的用字遣詞與圖表分析上老師也提供了許多寶貴的建議。老師如此負責與堅持的學術態度將會是學生心中永遠的榜樣。除此之外，口試期間還要特別感謝 陳柏中教授與蘇正耀教授的詳細審閱以及客觀的指正與建議，使得本論文能更加完備，在此由衷的獻上最深的感謝。

我還要感謝新物館 501 室的所有同學與學長。身為承接與黃琮暐學長碩士論文相關題目的我，不僅受到學長在學習研究上完整的照顧，並且在生活娛樂上學長也總是帶給我們歡樂。陳柏文學長也總是願意與我們討論研究上的問題並提供經驗談，讓我有與君一席話，勝讀十年書之感。簡崇欽學長本身努力不懈、專心致志的精神則是我做研究的榜樣。黃上瑜學長對研究問題一絲不苟的態度也是我一直由衷敬佩學習的對象。張晏瑞學長則總是照顧到我們的飲食育樂。另外，更要感謝與我同期共同奮鬥的蔡宇安同學，他不僅程式功力十分深厚，並時常給予我協助與討論外，其本身研究的熱忱更是我心中的楷模。而坐我旁邊的陳國進同學也常是與我聊天解悶的好對象。除此之外，港仔同學也一直是我們研究室的開心果，常常以獨特的人格特質帶給我們歡樂。

另外，也感謝我大學時期的好朋友們在我研究生涯中陪伴我度過許多歡笑的時光。蕭漁洋總是約我去兜風以幫助我紓解研究的壓力。陳巨軒奇妙的想法一直是 我好奇心的動力。王昱傑、廖乙碩是一路踢足球的最佳戰友。吳文正是懷抱著歷史情懷的天文學家。張天崑雖然低調卻默默吃香喝辣辦事有效率。虞姬一直是我們午飯團的招集人。 還有許多好朋友也都是支撐著我一路走來的原動力。

最後最感謝的是我的父母與我的女友季純(小寶)。如果沒有我父母從小到大的栽培與支持，我是不可能一路完成學業直到今天。我父親除了平常各類的小叮嚀外總是親自下廚給我吃，使我能有足夠的營養與健康的身體；我的母親則是在學習與工作上是我心中的榜樣，並且也時常給予我無私的支持。最後，因為有小寶的陪伴，我才能一路走過許多低潮與困難，小寶在我背後的打氣與支持一直是我最佳的後盾。更重要的是，小寶也是我的開心果，時常在困乏的研究生活中帶給我歡笑。

要感謝的人很多，掛一漏萬，若有遺漏在此也一併獻上內心最深的謝意。

中文摘要

量子邏輯閘 (Quantum Gate) 是在實際的物理上實現量子電腦最基本的元件。其中，固態的約瑟夫森量子元件 (Superconducting Josephson-Junction Qubit) 是實現量子邏輯閘最好的候選人之一。 而通常在面對建立量子邏輯閘的過程中，受環境影響的去相干化 (Decoherence) 和耗散 (Dissipation) 是最主要的課題。藉由克服此課題我們才有可能建造一個高準確度 (Fidelity) 且錯誤大約在$10^{-3} \sim 10^{-4}$ 之間的量子邏輯閘。因此，找尋一個好的操作策略來降低影響與建造量子邏輯閘是非常重要的。最佳化控制方法 (Optimal Control Method) 是其中一個有效的工具，並且已經被用在減少與環境的作用和建造高準度的量子邏輯閘上。另外，最佳化控制方法亦已經被拿來使用在假設環境與系統是沒有記憶效應的馬可夫開放系統 (Markovian Open Qunatum System) 上。但是，在諸多實際的相關實驗上，非同時的記憶效應 (Non-Local Memory Effect) 對於量子系統的影響是需要被關切的。尤其是在固態的裝置上環境的記憶效應是不可忽略的。所以，將最佳化控制方法延伸到在非馬可夫開放系統 (Non-Markovian Open Quantum System) 建立量子邏輯閘的研究是值得且具有必要性的。在本論文裡，我們首先回顧一些基礎的量子超導電路 (Superconducting Quantum Circuit) 並且介紹量子計算元件 (Quantum Qubit Device) 。接著，被視為解決最佳化問題其中一個最有效且恆定的計算方法—科羅多夫的最佳化控制方法 (Krotov Optimization Method) 將被引入。我們跟著推導非馬可夫開放系統以及含時的非馬可夫量子模型，並且將科羅多夫最佳化控制方法應用在非馬卡夫的單一量子邏輯閘 (Z-Gate)上。 並且發現控制相關係數 (Control-Dissipation Correlation) 和記憶效應 (the memory effect) 在高準確度的量子邏輯閘建立上，扮演極重要的角色。

Abstract

One of the fundamental criteria for physical implementation of a practical quantum computer is to design a reliable universal set of quantum gates. A promising class of candidates for realization of scalable quantum computers are solid-state quantum devices based on superconducting Josephson-junction qubits. Typically, a central challenge to overcome in this enterprise is decoherence and dissipation induced by the coupling to the its environment. It is thus important to find strategies to alleviate the problems and to to build a high-fidelity quantum gates meeting the error threshold of about $10^{-3} \sim 10^{-4}$. Optimal control method is one of the powerful tools already applied to the problem of dynamical decoupling from the environment and to finding the control sequence for high-fidelity quantum gates. Furthermore, optimal control technique has recently been applied to Markovian open quantum systems in which the approximation of the bath correlation function being delta-correlated in time is assumed. However, in some real experiments, we need to consider the non-local memory effects of the bath on the dynamics of the qubits. Especially, the bath memory effects are typically non-negligible in solid state devices. Thus it is desirable to apply optimal control technique to quantum gate operations in the non-Markovian open quantum systems. In this thesis, we first review some basic elements of superconducting quantum circuit and introduce the quantum qubit devices. We then introduce the Krotov optimization method which is one of the most effective and universal computation methods for solving optimal control problems. Then the quantum master equation approach for non-Markovian open quantum systems with time-dependent external control are presented. The Krotov based optimal method is then used to implement quantum logical gates for a single qubit in a non-Markovian environment. It is possible to achieve high-fidelity Z-gate with error less than 10^{-5} for the non-Markovian open qubit system. The control-dissipation correlation and the memory effect of the bath are crucial in achieving the high-fidelity gates.

Contents

List of Figures

List of Tables

Chapter 1

Introduction

In 1982 Feynman published a paper in which he discussed the question of whether it is possible to simulate quantum mechanics effectively using a classical (probabilistic) computer. He also introduced the concept of a quantum computer as a universal quantum simulator which uses "quantum elements" in order to simulate another quantum system. For a quantum computer, such a quantum element is a *quantum bit* or *qubit*, which can be seen as the quantum mechanical analogue to the classical bit. The difference with respect to the classical bit, which is either in the state 0 or 1, is that a qubit can be in a superposition state. The relevant idea of a quantum computer that make use of superposition, interference entanglement or other quantum effects based on the principles of quantum mechanics was introduced by Deutsch in 1985. The power of quantum computing in factoring and discrete logarithm was proposed by Shor in 1994. After two years, Grove published an quantum algorithm for searching an unordered database. These quantum algorithms make possible to solve those problems which are difficult to solve with classical computers.

To achieve the purpose of quantum computing and quantum information, practical *quantum bits* or *qubits* to perform reliably single- and two-qubit gates are needed. Various candidates for realizing building quantum bits have been proposed in the last decade. Intensive experimental and theoretical activities to realize suitable schemes for quantum gates in a variety of physical systems such as ion traps, cold atoms and solid-state devices were reported. One of the most promising class of candidates is solid-state quantum devices based on superconducting Josephson-junction qubits. Series of ingenious experiments related to superconducting qubit have been demonstrated and theoretical proposals have been investigated. Fundamentally, a quantum system is never completely isolated from its environment which results in noticeable effects such as decoherence, dissipation, and entanglement. One prominent example embodies a two-level system interacting with a collection of harmonic oscillators, the so-called spin-boson model. Many works were

recently directed toward understanding and controlling the dissipative spin-boson dynamics in nonequilibrium situations such as applying time-dependent external fields to build a quantum gate. In the related experiments[] the measured fidelity was increased up to 87% via accounting for measurement errors and large decoherence times. However, the requirement for high fidelity gates with error less than 10^{-3} for the purpose fault-tolerant quantum computation has not be done. Therefore it is important to find strategies to alleviate the effects of environments and to build quantum gates through time-dependent controls.

Optimal control method is one of the powerful tools already applied to the problem of dynamical decoupling from the environment and to finding the control sequence for high-fidelity quantum gates. Furthermore the optimal control method based on Krotov's method is proved to satisfy sufficient and necessary conditions and can find the global minimum or maximum for the given initial values. It has also been extended to treat quantum systems with noise, imperfections and leakage to noncomputational states [16, 30, 25]. Besides, optimal control technique has recently been applied to Markovian open quantum systems in which the approximation of the bath correlation function being delta-correlated in time is assumed [22]. However, in some real experiments, we need to consider the non-local memory effects of the bath on the dynamics of the qubits. Especially, the bath memory effects are typically non-negligible in solid state devices. Thus it is desirable to apply optimal control technique to quantum gate operations in the non-Markovian open quantum systems [6, 29, 20, 4, 7, 8].

In this thesis, we will investigate quantum optimal control problem for superconducting qubits using optimization method based on Krotov's method [10]. In chapter 2, we begin with a brief introduction of the Josephson Effect and discuss the physical properties of the Josephson junction. Then, the cooper-pair box and the SQUID quantum devices are introduced. These devices play the fundamental roles in recent physical research. Finally, charge qubits and flux qubits are discussed, which are the most important elements for quantum computing and information processing.

In chapter 3, we start from the original Krotov's optimal method, and then summarize the algorithm of achieving the optimal control process. Few examples are given to illustrate and demonstrate the optimal control method. An optimal control case on a closed quantum system is also discussed for the purpose of further extension.

In chapter 4, the theory of quantum master equation used to describe open quantum system dynamics is introduced. The Born approximation and Markov approximation are discussed. We also use the Born approximation to obtain the master equation for a time-dependent non-markovian open quantum system which will be used in our problems. Moreover, the useful tricks for dealing with open quantum systems are discussed.

Finally, In chapter 5, we will the Krotov based optimal control method to investigate the quantum optimal control problem of the quantum gate operations for superconducting qubits. We first introduce the novel form of equations of motion of the open quantum system we study, and extend the optimal control method to the equation. We obtain optimal control sequences for the single-qubit gate, including the Z-gate in the presence of a non-Markovian environment.

Chapter 2

Superconducting Quantum Qubit

2.1 Josephson Junctions

The phenomenon that electric current across two weakly coupled superconductors is called Josephson effect. British physicist Brian David Josephson predicted the existence of the effect in 1962. Josephson Effect is one of the most important discover in the last century. It not only open a new physical field for fundamental interesting but also shows a long-term potential on quantum computing and quantum technology[3, 34, 13, 12, 9, 27]. The superconducting circuits built by Josephson junction has generic quantum properties such as quantized energy level, entanglement and superposition of states, all of which are more easier connected with atoms. On the other hand, these circuits can be designed and constructed to control their characteristic frequencies and other parameters. These frequencies and parameters can be adjusted by controlling an external magnetic field ,voltage and current. This possibilities can be extended to the idea of quantum bits(qubits)[3, 34, 13, 12], which are the fundamental elements of quantum computer. In this chapter, we begin with a brief introduction of Josephson Effect and discussing the physical qualities of the Josephson junction. Secondly, the cooper-pair box and the SQUID quantum devices are introduced. These devices play the fundamental characters in recent physical research. Finally, charge qubits and flux qubits are discussed, which are the most important elements for quantum computing and quantum communication.

2.1.1 Josephson Effect

Consider two superconductors separated by a macroscopic distance. In the situation, the phase of the two superconductors can change independently. When the two superconductors are moved closer, so that their separation is reduced to about 30 Å, quasiparticles can flow from one superconductor to the other by means of tunnelling. If we further reduce

the distance between two superconductors down to 10 Å, as we shall see, also Cooper pairs can flow from one superconductor to the other, this phenomenon is called Josephson tunnelling. One can build a Josephson junction which consists of a sandwich of two superconductors separated by a thin insulating layer to see the Josephson tunnelling effect. In the experiment, current and voltage can be changed, so there are two kind of Josephson effect: DC Josephson effect and AC Josephson effect. DC Josephson effect is happened when a DC current flows across the junction in the absence of any electric or magnetic field. The relationship between the phase difference δ and the current I of superconducting pairs across the junction is

$$I_J = I_c sin\delta \tag{2.1}$$

The critical current I_c is the maximum zero-voltage superconducting current that can pass through the junction above which the superconducting state will become normal state. It is proportional to the transfer interaction. Because no voltage apply, the phase difference δ is a constant. For finite voltage situations involving the AC Josephson effect, a more complete description is required. AC Josephson effect is happened when a DC voltage is applied across the junction, an AC current flows across the junction. The phase difference δ is no longer a constant. The relationship between voltage and phase difference is

$$\dot{\delta} = -2eV/\hbar \tag{2.2}$$

or

$$\delta(t) = -\frac{2e}{\hbar}\int_0^t V dt + \delta(0) \tag{2.3}$$

and the superconducting current is

$$I_J = I_c sin(\delta(0) - 2eVt/\hbar) \tag{2.4}$$

Furthermore, considering more general cases, we can apply a time-dependent voltage, and write down the function in some significant symbols,

$$I_J(t) = I_c sin\frac{\Phi(t)}{\phi_0} = I_c sin\delta(t) \tag{2.5}$$

where the generalized flux is defined by $\Phi_J = \int_\infty^t V(t')dt$ and $\phi_0 = \hbar/2e$ is the reduced flux quantum, or $\phi_0 = \Phi_0/2\pi$, where $\Phi_0, h/2e$, is the magnetic flux quantum. Actually, phase difference is not a gauge-invariant quantity; for a given physical situation, there is not only one unique value of phase difference. Hence it cannot in general determine the current I_J, which is a well-defined gauge-invariant physical quantity. The phase difference mentioned before is not the real phase difference between two superconductor, defined by

$$\delta \equiv \delta' - \frac{2\pi}{\Phi_0}\int \vec{A}\cdot\vec{dl} \tag{2.6}$$

where δ' is the real phase difference and the integration over the vector potential $\vec{A}$ is from one electrode of the weak link to the other. Thus, the difficulty is cured. In addition to curing the conceptual problem, the introduction of the gauge-invariant phase difference is the key to working out the effects in a magnetic field, which cannot be treated without introducing the vector potential $\vec{A}$.

For some cases, one need to consider a Josephson junction with a nonlinear inductance. At first, let's take a short review of a conventional inductance.

$$L = \Phi/I \text{ or } I = \phi/L, \tag{2.7}$$

where L is the inductance, Φ is the magnetic flux, and I is the current, We thus expand Eq. (2.5)

$$I_J = \frac{1}{L} - \frac{1}{6L_J\phi_0^2}\Phi_J^3(t) + ... \tag{2.8}$$

or simpletly

$$I_J(t) = I_c sin\delta(t) = I_c(\delta(t) - \frac{\delta^3(t)}{3!}) \tag{2.9}$$

By comparing the functions of a Josephson junction and a conventional inductance, it is very easy to find that besides the linear term in the relation of current and magnetic flux, there are additional nonlinear high-order terms in a Josephson junction. A Josephson junction, therefore, can be considered having a nonlinear inductance.

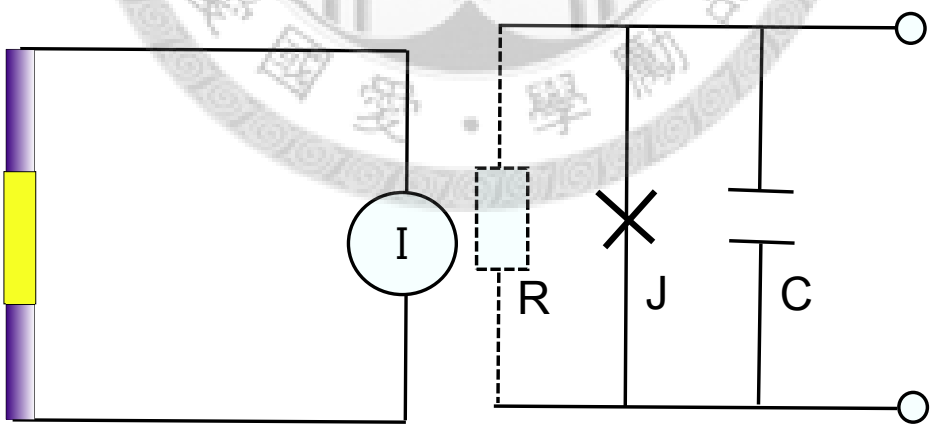

Figure 2.1: The current-biased Josephson junction and its equivalent circuit.

2.1.2 The current-biased Josephson junction

A Josephson junction schematically shown in Fig. 2.1 as a sandwich structure can be modeled as a parallel circuit which consists of a nonlinear inductance, a resistance, and

a capacitance. According to Kirchhoff's rule and some relationships, $I = C\dot{V} = C\ddot{\delta}$, $\delta = \frac{2e}{\hbar}\Phi$ and $I_j = I_c sin\delta$, the equation of the circuit is

$$\frac{\hbar}{2e}C\ddot{\delta} + \frac{\hbar}{2eR}\dot{\delta} + I_c sin\delta = I_e, \tag{2.10}$$

where C is the capacitance, R is the resistance, and V is the voltage across the capacitance. Then, it is useful to define some meaningful parameters, $Ec \equiv \frac{4e^2}{2C}$ and $E_J \equiv \frac{\hbar}{2e}I_c$. The kinetic energy of the quasi-partial of phase δ is

$$K(\dot{\delta}) = \frac{\hbar^2\dot{\delta}^2}{4E_c}, \tag{2.11}$$

the potential energy of it is

$$U(\delta) = E_J(1 - cos\delta) - \frac{\hbar}{2e}I_e\delta, \tag{2.12}$$

and the Hamiltonian has the form

$$H = E_C n^2 - E_J cos\delta - \frac{\hbar}{2e}I_e\delta, \tag{2.13}$$

The relationship of potential versus phase is shown in Fig. 2.2. It is obvious that nonlinear inductance, $cos\delta$, makes potential oscillate and bias current makes it slope. When current bias is applied, the pendulum potential becomes tilted. By the way, a current-biased Josephson junction can be considered as a qubit, because the potential is cosine function, making energy gaps different.

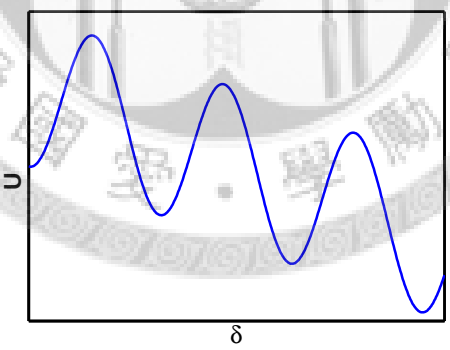

Figure 2.2: The "tilted-washboard" effective potential versus phase difference of a current-biased Josephson junction.

2.2 The Cooper-pair box and the SQUID

2.2.1 The single cooper-pair box device

There is a small superconducting island in a superconducting Cooper-pair box(SCB) device as shown in Fig. 2.3. One side of the island is connected via a Josephson tunneling

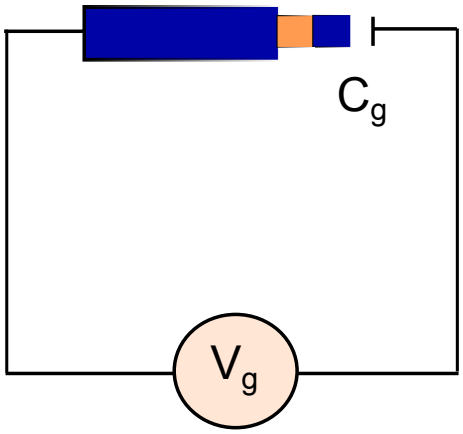

Figure 2.3: The single Cooper pair box. One side of a small superconducting island is connected via a Josephson tunnel junction to a large superconducting reservoir, and another side is coupled capacitively to a voltage source.

junction to a large superconducting reservoir, and the other side is coupled capacitively to a voltage source. Cooper pair can only transfer to the island one by one in the device. The number of electrons on the island is controlled by the bias voltage.

The Hamiltonian of the cooper-pair box is

$$\hat{H} = E_C(\hat{n} - n_g)^2 - E_J cos\hat{\delta} \tag{2.14}$$

where $n_g = C_g V_g/2e$ is the offset Cooper pair number caused by the gate voltage V_g through gate capacitance C_g, and n is the number of extra Cooper pairs between the two capacitances, the gate capacitance and the capacitance in the Josephson junction. Therefore, the first term, $E_C(\hat{n} - n_g)^2$, represents the electrostatic energy of the island, where $E_C = 4e^2/2(C + C_g)$. Due to the nonlinear inductance of the Josephson junction, the second term, $E_J cos\hat{\delta}$, appears.

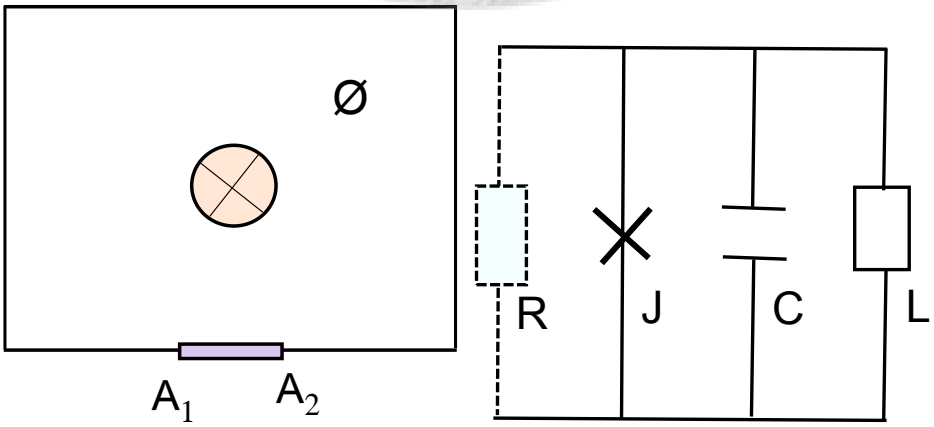

Figure 2.4: The superconducting quantum interference device, SQUID, and its equivalent circuit.

2.2.2 The SQUID device

A Superconducting quantum interference device(SQUID) is a device involved with quantum interference. A rf-SQUID, shown in Fig. 2.4, consists of a superconducting loop interrupted by a tunnel junction. a external magnetic flux is sent through the loop, inducing quantum interference. According to the Meissner effect, we have

$$J(\vec{r}) = |\Psi(r)|^2[\frac{q\hbar}{m*}\nabla\theta(\vec{r}) - \frac{q^2}{m*c}\vec{A}(\vec{(}r))] \tag{2.15}$$

where $\vec{A}$ is the vector potential and $q \equiv -2e$ for a Cooper pair. Inside a superconductor, the current vanlishs,

$$\nabla\theta(\vec{r}) = -\frac{2e}{\hbar c}\vec{A}(\vec{r}) \tag{2.16}$$

Choosing a contour inside the superconducting loop. with Eq. (2.6) we can get

$$\begin{aligned}\Phi_t &= \oint_c \vec{A}\cdot d\vec{l} = \int_{A_1}^{A_2}\vec{A}\cdot d\vec{l} + \int_{A_2}^{A_1}\vec{A}\cdot d\vec{l} \\ &= -\frac{2e}{\hbar c}\int_{A_1}^{A_2}\nabla\theta(\vec{r})\cdot d\vec{l} + \int_{A_1}^{A_2}\vec{A}\cdot d\vec{l} \\ &= \frac{2e}{\hbar c}\delta,\end{aligned} \tag{2.17}$$

where Φ_t is total manetic flux.

With magnetic flux $\Phi = \Phi_t - \Phi_e$ where Φ_e is external magnetiv flux and the inductance energy $\frac{\Phi^2}{2L}$, the Hamiltonian of a rf-SQUID is given by

$$\hat{H} = E_C\hat{n}^2 - E_J cos\hat{\delta} + E_L\frac{(\hat{\delta}-\delta_e)^2}{2} \tag{2.18}$$

where $\delta_e = \frac{2e}{\hbar}\Phi_e$. The first term $E_C\hat{n}^2$ is electrostatic energy of the capacitance in the Josephson junction, and the second term is related to the Josephson energy. The last term corresponds to the inductance energy of the loop, and $E_L = \frac{\Phi_0^2}{4\pi^2 L}$.

Now we introduce another SQUID device called dc-SQUID. A dc-SQUID is a device which consists of two tunnel junction in a superconducting loop and is biased by an external current. It is similar to a current-biased Josephson junction with a two-junction loop, as shown in Fig. 2.5, instead of a single junction. Two superconducting phases, $\delta_{1,2}$, is involved, and according to Eq.(2.5), the external current is

$$I_{c1}sin\delta 1 - I_{c2}sin\delta_2 = I_e \tag{2.19}$$

It is convenient to define some new variables,

$$\delta_\pm = \frac{\delta_1 \pm \delta_2}{2} \tag{2.20}$$

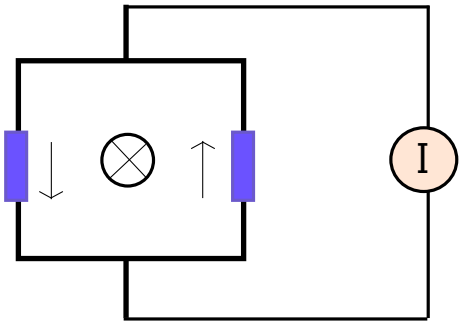

Figure 2.5: The dc-SQUID. A superconducting loop with two Josephson junctions replaces the single junction in the current-biased Josephson junction circuit.

and in a symmetry case, which the two Josephson junction are the same $I_{c1} = I_{c2}$ Eq.(2.19) reduces to the form

$$2I_c cos(\delta_e/2) sin\delta_- = I_e \tag{2.21}$$

Comparing Eq. (2.21) with Eq. (2.5), we can find that $2I_c cos(\delta_e/2)$ is the effective critical current. Most importantly, it can be tuned by the external magnetic flux and consequently the effective Josephson energy, $E_J = \frac{\hbar}{2e} 2I_c cos(\delta_e/2)$ is tunable too. The Hamiltonian can be written by generalizing Eqs. (),() for the phases $\delta_\pm$.

$$\begin{aligned} H &= E_C \hat{n}_+^2 + E_c \hat{n}_-^2 - 2E_J cos\hat{\delta}_+ cos\hat{\delta}_- \\ &\quad + E_L \frac{(2\hat{\delta}_+ - \delta_e)^2}{2} + \frac{\hbar}{2e} I_e \hat{\delta}_-, \end{aligned} \tag{2.22}$$

where $\hat{n}_+$ and $\hat{n}_-$ are the conjugate momentum of $\hat{\delta}_+$ and $\hat{\delta}_-$. According to quantum mechanics-just like the familiar position and momentum operators $\hat{x}$ and $\hat{p}_x$-the operator $\hat{\delta}$ and Cooper-pair number operator $\hat{n}$ on the capacitor are canonically conjugate, as expressed by the commutator braket, $[\hat{\delta}, \hat{n}] = i$.

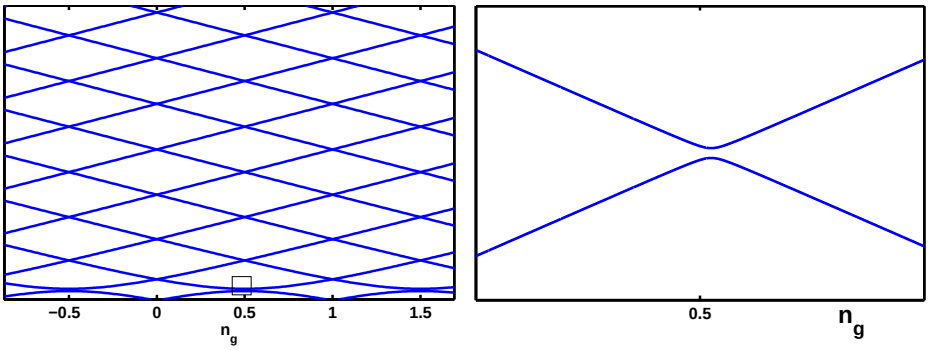

Figure 2.6: Left: The energy spectrum of a charge qubit versus gate voltage. Right: The lowest two energy levels near $V_g = 0.5$, the part circumscribed by solid line in left figure.

2.3 Charge Qubits and Flux Qubits

2.3.1 Charge qubits

A superconducting Josephson junction qubit in which the charging energy is much large than the Josephson coupling, $E_C >> E_J$, is called a charge qubit. In this regime, a convenient basis is formed by the charge states, and the phase terms can be considered as perturbation. This is why this kind of qubits are called charge qubits. The necessary of one-qubit and two-qubit gates can be performed by controlling applied gate voltages and magnetic fields. Different designs will be presented that not only complexity, but also in flexibility of manipulations. In this subsection, the simplest charge qubit, cooper-pair box, Fig. 2.3, is presented in details. This is example illustrates how charge qubits provide two energy states, which satisfy the requirement of qubits. In charge regime, at first we expand all operators in the basis of the charge states $\{|n\rangle\}$. The Hamiltonian of a cooper-pair box, Eq. (2.14), is

$$\hat{H} = E_C(\hat{n} - n_g)^2 - E_J cos\hat{\delta}. \tag{2.23}$$

Then by using the properties of orthonomal and complete set, $\langle n|\hat{n}|n'\rangle = \delta_{n,n'}$ and $I = \sum_n |n\rangle\langle n|$, the first term is rewritten as

$$\sum_n E_C(n - n_g)^2 |n\rangle\langle n| \tag{2.24}$$

and by using the commutator relation,

$$\begin{aligned} & [\hat{\delta}, \hat{n}] = i, \\ \Rightarrow \quad & [\hat{\delta}^m, \hat{n}] = im\hat{\delta}^{m-1}, m > 0 \\ \Rightarrow \quad & [\hat{n}, e^{i\hat{\delta}}] = [\hat{n}, \sum_m \frac{(i\hat{\delta})^m}{m!}] = e^{i\hat{\delta}} \end{aligned} \tag{2.25}$$

The commutator relation Eq. (2.25) is similar to the commutator relation of number operator $\hat{a}^\dagger\hat{a}$ and the creation operator $\hat{a}^\dagger$, $[\hat{a}^\dagger\hat{a} = \hat{a}^\dagger$. so $e^{i\hat{\delta}}$ and $e^{-i\hat{\delta}}$ can be presented in charge basis,

$$e^{i\hat{\delta}} = \sum_n |n+1\rangle\langle n|, e^{-i\hat{\delta}} = \sum_n |n\rangle\langle n+1| \tag{2.26}$$

and the second term of Eq. (2.14) is

$$\frac{1}{2}E_J \sum_n (|n\rangle\langle n+1| + |n+1\rangle\langle n|). \tag{2.27}$$

By combining Eq. (2.24) and Eq. (2.27), in this basis the Hamiltonian reads

$$\begin{aligned} \hat{H} = & \sum_n \{E_C(n - n_g)^2 |n\rangle\langle n| - \\ & \frac{1}{2}E_J(|n\rangle\langle n+1| + |n+1\rangle\langle n|)\} \end{aligned} \tag{2.28}$$

The energy spectrum of Eq. (2.28) is shown in Fig. 2.6:left Under suitable conditions, when charge number on a gate capacitor n_g controlled by gate Voltage V_g equals half integers, the lowest two energy states are well-isolated from other states, shown in Fig. 2.6:right Because of that, near $n_g = 1/2$, the Hamiltonian can be reduced to

$$\hat{H} = -\frac{1}{2}(\epsilon\sigma_z + \Delta\sigma_x), \tag{2.29}$$

where $\epsilon = E_C(1 - 2n_g)$, and $\Delta = E_J$. The qubit eigenenergies are then given by the equation

$$E_{1,2} = \mp\frac{1}{2}\sqrt{E_C^2(1 - 2n_g)^2 + E_J^2}. \tag{2.30}$$

So, under suitable conditions charge qubits provide physical realizations of qubits with two charge states differing by one cooper-pair charge on a small island. For quantum computation, it is required to have the ability to rotate a state on the Bloch sphere to any position at will, and consequently σ_z and σ_x rotation are necessary. In a cooper-pair box, pure σ_x rotation is acquirable, as $n_g = 1/2$, but pure σ_z rotation is not, since E_J is fixed. In previous part, an important concept is mentioned. A two-junction loop can substitute for the single Josephson junction, creating a SQUID-controlled qubit, Fig. 2.7. Thus, the effective Josephson energy E_J is tunable and pure σ_z rotation can be performed.

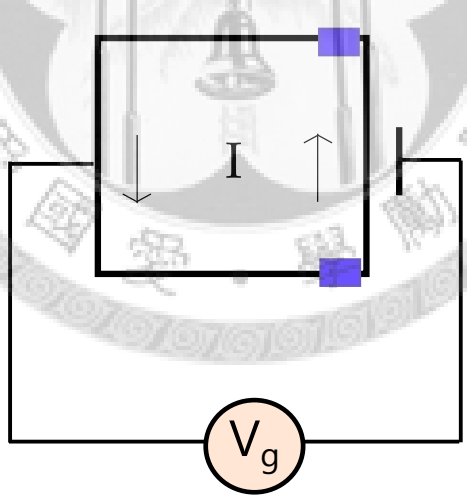

Figure 2.7: The single Cooper pair transistor. A superconducting loop with two Josephson junctions replaces the single junction in a SCB for a tunable E_J.

2.3.2 Flux qubits

In the previous section, we describe the quantum dynamics of low-capacitance Josephson devices where the charging energy dominates over the Josephson energy, $E_C >> E_J$, and the relevant quantum degree of freedom is the charge on superconducting island. We

do talk about another quantum regime, the phase regime, $E_J >> E_C$, in which the flux states are the better basis. This kind of qubits are called flux qubits. A rf-SQUID is the simplest example of a flux qubit. The Hamiltonian Eq. (2.18) is

$$\hat{H} = E_C\hat{n}^2 - E_J cos\hat{\delta} + E_L\frac{(\hat{\delta}-\hat{\delta}_e)^2}{2}, \tag{2.31}$$

and in the phase regime, the potential energy is given by

$$U(\delta) = -E_J cos\delta + E_L\frac{(\delta-\delta_e)^2}{2}. \tag{2.32}$$

The potential energy is cosine function added a second power function. δ_e in a flux qubit play as the same role as n_g do in a charge qubit. The lowest area can be approximated to a double-well. When δ_e equals π or odd π, a symmetric double-well potential energy appears. It is similar to that of n_g equal 1/2 in a charge qubit. Because of the tunnelling through center barrier, the lowest two energy level split with a gap Δ, which depends on the height of the barrier. When δ_e does not equal π or odd π, the potential energy becomes unsymmetric, the probability of the lowest energy pair is not half in each well. This situation is like when n_g is near 1/2, in a charge qubit, the probability is not the same in $|0\rangle$ and $|1\rangle$. The Hamiltonian of a flux qubit can be truncated to the lowest two energy states in a simple form of

$$\hat{H} = -\frac{1}{2}(\epsilon\sigma_z + \Delta\sigma_x), \tag{2.33}$$

where Δ depends on E_J and ϵ is given by

$$\epsilon = 4\pi\sqrt{6(E_J/E_C - 1)}E_J(\Phi_e/\Phi_0 - 1/2). \tag{2.34}$$

In this form, the pure operator X-rotation can be performed by setting $\Phi/\Phi_e = 1/2$, but the pure Z-rotation can not. In order to solve this problem, we can replace the single junction with a two-junction loop that introduces an additional external flux Φ_e as another control variable. Therefore, the effective Josephson energy becomes tunable.

Chapter 3

Krotov Optimal Control Method

3.1 Preliminary Preparation of the Krotov Method

In the Krotov optimal control method, one need to know the equation of motion of a system, and decide the goal (cost) function for the system. The goal function depends on the function of system and the control parameters. For further implementation, we consider the equation of motion to be of the form

$$\frac{\partial x}{\partial t} = v[t, x(t), c(t)], \tag{3.1}$$

and suppose we want to minimize the general form of the goal function

$$I[x(t), c(t)] = \int_0^T f^0(t, x(t), c(t))dt + F[x(T)] \longrightarrow \min. \tag{3.2}$$

Here $x(t)$ is the system evolution function with time or the trajectory of the system, $c(t)$ is the control parameter with time, and the vector-functional $f^0(t, x(t), c(t))$ and the functional $F[x(T)]$ are defined for all $t, x(t), c(t)$ and are twice differentiable with respect to t and x. The initial vector $x(0) = x_0$ is a given and fixed vector, $x(T)$ is the final values of the vector $x(t)$ at final time T, and $c(t)$ can be required within a close set U. The general functional, $F[x(T)]$, depends only on the final value of $x(t)$ and $f^0(t, x(t), c(t))$ depends on the intermediative values of $x(t)$ and $c(t)$, so $F[x(T)]$ and $f^0(t, x(t), c(t))$ are general functional that representing that the goal function I depends on the terminal and intermediate time values of $x(t)$. For a quantum system with multi-dimensional vector space or multi-argument processes and control parameters, we will have more than one equation of motion, $\dot{x}^i(t) = v^i[t, x^i(t), c^i(t)]$, and the minimization problem will become to $I[t, x^i(t), c^i(t)] = \int_0^T f^0[t, x^i(t), c^i(t)] + F[x^i(t)]$, where $i = 1, 2, ..., n$.

3.2 The Tricks of Krotov Method

3.2.1 Decomposition of Goal Function

For implementing the Krotov method, a real and twice differentiable function $\phi[t, x(t)]$ is introduced. The function can be proved to satisfy the constructions

$$R[t, x(t), c(t)] = \frac{\partial \phi}{\partial x} v[t, x(t), c(t)] - f^0[t, x(t), c(t)] + \frac{\partial \phi}{\partial t}, \tag{3.3}$$

$$G[T, x(T)] = F[T, x(T)] + \phi[T, x(t)], \tag{3.4}$$

$$L[x(t), c(t), \phi] = G[T, x(T)] - \int_0^T R[t, x(t), c(t)]dt - \phi[0, x(0)]. \tag{3.5}$$

To be more specific, $L[x(t), c(t), \phi] = I[t, x(t), c(t)]$ for any function $\phi[t, x(t)]$ and all of the $x(t)$ and $c(t)$ can be shown through the constructions. The following is the proof:

$$\begin{aligned}
L[x(t), c(t), \phi] &= G[T, x(T)] - \int_0^T R[t, x(t), c(t)] - \phi[0, x(0)] \\
&= G[T, x(T)] - \int_0^T [\frac{\partial \phi}{\partial x} v[t, x(t), c(t)] - f^0[t, x(t), c(t)] + \frac{\partial \phi}{\partial t}]dt \\
&\quad -\phi[0, x(0)] \\
&= G[T, x(T)] - \int_0^T [\frac{\partial \phi}{\partial x}\frac{dx}{dt} + \frac{\partial \phi}{\partial t} - f^0[t, x(t), c(t)]]dt \\
&\quad -\phi[0, x(0)] \\
&= F(T, x(T)) + \phi(T, x(T)) - \int_0^T \frac{d\phi}{dt}dt - \phi[0, x(0)] \\
&\quad + \int_0^T f^0[t, x(t), c(t)]dt \\
&= F(T, x(T)) + \int_0^T f^0[t, x(t), c(t)]dt \\
&= I[t, x(t), c(t)].
\end{aligned} \tag{3.6}$$

Therefore minimizing $I[t, x(t), c(t)]$ can be achieved by minimizing $L[t, x(t), c(t), \phi]$, and this intends to minimizing $G[x(T)]$ and maximizing $R[t, x(t), c(t)]$.

For a multi-dimensional quantum system or multi-argument processes, the equations of R and G will be written as $R[t, x^i(t), c(t)] = \frac{\partial \phi}{\partial x^i} v[t, x^i(t), c(t)] - f^0[t, x^i(t), c(t)] + \frac{\partial \phi}{\partial t}$ and $G[T, x^i(T)] = F[T, x^i(T)] + \phi[T, x^i(T)]$. For later use, it is convenient to define the function $\Phi = \frac{\partial \phi}{\partial t}$, and the functional $R[t, x^i(t), c(t)] = H[t, x^i(t), c(t), \Phi(t)] + \frac{\partial \phi}{\partial x^i}$, where

$$H[t, x^i(t), c(t), \Phi(t)] = \Phi v[t, x^i(t), c(t)] - f^0[t, x^i(t), c(t)]. \tag{3.7}$$

Note that the parameters in H denoted by Φ emphasize that x^i and $\frac{\partial \phi}{\partial x^i}$ should be treated as independent variables with respect to H.

3.2.2 Iterative Algorithm of the Krotov Method

The main purpose of the Krotov method is to find out optimal control sequences $c_{k+1}(t)$ in $k+1$ iteration can perform better than k iteration. In other words, Krotov method hopes $I[t, x(t), c(t)]$ is monotonically decreasing respect to $c_k(t)$ when k is increasing. That is, $I[t, x_k(t), c_k(t)] \geq I[t, x_{k+1}(t), c_{k+1}(t)]$ in every iteration. Since $\phi[t, x(t)]$ is not restricted, we can freely choose the form of $\phi[t, x(t)]$. However, if we can construct the function $\phi[t, x(t)]$ to make $L[t, x_k(t), c_k(t), \phi]$ being maximized in each k then we can randomly choose next control sequences $c_{k+1}(t)$ without worrying about the effect of $c(t)$ will increase the value of $L[t, x(t), c(t), \phi]$. We therefore derive a smaller value of the goal function by the chosen ϕ. To be more clearly, we suppose that we already found the function ϕ for a problem, and the complete processes will be as follows:

(i.) Taking an arbitrary control sequences $c_0(t)$ and than deriving the corresponding trajectory $x_0(t)$.

(ii.) Choosing the functional $\phi[t, x(t)]$ to make $L[t, x(t), c(t), \phi]$ a maximum with the control $c_0(t)$ and trajectory $x_0(t)$. This requirement is equivalent to the following two conditions:

$$R[t, x_0(t), c_0(t)] = \min_x R[t, x(t), c_0(t)], \tag{3.8}$$

$$G[T, x(T)] = \max_x G[T, x(T)]. \tag{3.9}$$

Above conditions imply that the functional R and G are calculated using the new $\phi[t, x(t)]$. As a result, the current control sequences $x_0(t)$ will be the worst of all possible $x(t)$ in minimizing the goal functional $L[t, x(t), c(t), \Phi] = I[t, x(t), c(t)]$. Any change in $c(t)$ which makes a new trajectory $x(t)$ will now improve the minimization of the goal function $I[t, x(t), c(t)]$.

(iii.) Finding a new control sequences $\tilde{c}(t)$ that maximizes the functional R. The corresponding conditions are

$$\begin{aligned} \tilde{c}[t, x(t)] &= Arg \max_c R[t, x(t), c(t)] \\ &= Arg \max_c H[t, x(t), c(t), \Phi], \end{aligned} \tag{3.10}$$

where H is mentioned in Eq. (3.7). Note that the control sequences $\tilde{c}[t, x(t)]$ depends on the trajectory function $x(t)$.

(iv.) With the new control sequences $\tilde{c}[t, x(t)]$ the new trajectory $x_1(t)$ can be derived by the equation of motion of Eq. (3.1).

(v.) It is now guaranteed that the goal function in Eq. (3.2) has been minimized monotonically, which can be written as $I[t, x_1(t), c_1(t)] \leq I[t, x_0(t), c_0(t)]$. The new control sequences and the trajectory become a starting point of the next iteration and (i.)-(iv.) can be repeated for the further decreasing in the goal function.

3.2.3 Monotonically Convergence of Krotov Method

Now we prove the new $I[t, x^1(t), c^1(t)]$ indeed smaller than the previous $I[t, x_0(t), c_0(t)]$. It is straightforward to show that

$$\begin{aligned}
\Delta I &= I[t, x_0(t), c_0(t)] - I[t, x_1(t), c_1(t)] \\
&= L[t, x_0(t), c_0(t), \Phi] - L[t, x_1(t), c_1(t), \Phi] \\
&= \int_0^T R[t, x_1(t), c_1(t)] - R[t, x_1(t), c_0(t)]dt + G[T, x_0(T)] - G[T, x_1(T)] \\
&= \Delta_1 + \Delta_2 + \Delta_3 \qquad (3.11)
\end{aligned}$$

where

$$\Delta_1 = G[T, x_0(T)] - G[T, x_1(T)] \qquad (3.12)$$

$$\Delta_2 = \int_0^T R[t, x_1(t), c_1(t)] - R[t, x_1(t), c_0(t)]dt \qquad (3.13)$$

$$\Delta_3 = \int_0^T R[t, x_1(t), c_0(t)] - R[t, x_0(t), c_0(t)]dt. \qquad (3.14)$$

Using the conditions in Eq. (3.8) and Eq. (3.9) one can prove that $\Delta_1 \geq 0$ and $\Delta_3 \geq 0$, and Eq. (3.10) also guarantee $\Delta_2 \geq 0$. Therefore the new goal functional I will be smaller than the previous one and the monotonically convergence has been proved.

3.3 Construction of ϕ

To carry out the above iteration method, the most important and hardest task is finding a ϕ that satisfies the conditions in Eq. (3.8) and Eq. (3.9) which require the absolute maximum of the functional R and minimum of the functional G of the old control sequences $c_0(t)$ and the old trajectory $x_0(t)$. In this section, we will show how to construct ϕ in first order to x and in second order to x to cope with lineaer and non-lineaer problems.

3.3.1 First Order in x

If the equations of motion of the system are linear and can be written as

$$\frac{\partial x^i}{\partial t} = v^i[t, x(t), c(t)] = a^i_j[t, c(t)]x^j + b^i, \ i = 1, 2, ..., n, \qquad (3.15)$$

and the function $f^0[t, x(t), c(t)]$ and $F[x(T)]$ are concave with respect to $x(t)$, which means

$$\frac{\partial^2 f^0[t, x(t), c(t)]}{\partial x^i \partial x^i} \leq 0, \qquad \frac{\partial^2 F[T, x(T)]}{\partial x^i(T) \partial x^i(T)} \leq 0. \tag{3.16}$$

In this case, we just need to consider ϕ in first order to x since the second derivative is guaranteed. To be more specific, The first order that implies the functional ϕ needs to satisfy Eq. (3.8) and Eq. (3.9) but do not have to worry about the second derivative of the function R and G. Therefore the function ϕ only need to fit the conditions that the first derivative of the functions R and G are equal to zero. For the reasons, we can choose the function $\phi[t, x^i(t)] = \Phi^i(t)x^i(t)$ which satisfies the following conditions:

$$\begin{aligned}
\frac{\partial R(t, x_0, c_0)}{\partial x} &= \frac{\partial^2 \phi(t, x_0)}{\partial x^2} f(t, x_0, c_0) + \frac{\partial \phi}{\partial x} \frac{\partial f(t, x_0, c_0)}{\partial x} - \frac{\partial f^0(t, x_0, c_0)}{\partial x} \\
&\quad + \frac{\partial}{\partial t} \frac{\partial \phi(t, x_0)}{\partial x} \\
&= \frac{\partial H(t, x_0, c_0, \Phi)}{\partial x} + \frac{\partial^2 \phi(t, x_0)}{\partial x^2} f(t, x_0, c_0) + \frac{\partial}{\partial t} \frac{\partial \phi(t, x_0)}{\partial x} \\
&= \frac{\partial H(t, x_0, c_0, \Phi)}{\partial x} + (\frac{\partial x}{\partial t} \frac{\partial}{\partial x} + \frac{\partial}{\partial t}) \frac{\partial \phi(t, x_0)}{\partial x} \\
&= \frac{\partial H(t, x_0, c_0, \Phi)}{\partial x} + \frac{d\Phi(t, x_0)}{dt} \\
&= 0,
\end{aligned} \tag{3.17}$$

$$\begin{aligned}
\frac{\partial G(x, x_0(T))}{\partial x(T)} &= \frac{\partial F(x_0(T))}{\partial x(T)} + \frac{\partial \phi(T, x_0(T))}{\partial x(T)} \\
&= \frac{\partial F(x_0(T))}{\partial x(T)} + \Phi(T, x_0(T)) \\
&= 0.
\end{aligned} \tag{3.18}$$

Therefore, Eq. (3.17) is the equation of motion for the function Φ :

$$\frac{\partial \Phi}{\partial t} = -\frac{\partial H[t, x_0, c_0, \Phi]}{\partial x} \tag{3.19}$$

with boundary conditions Eq. (3.18)

$$\Phi(T, x_0(T)) = \frac{\partial F(T, x_0(T))}{\partial x(T)} \tag{3.20}$$

given by Eq. (3.18)and from Eq. (3.1) and Eq. (3.7)

$$\frac{\partial x}{\partial t} = \frac{\partial H[t, x_0, c_0, \Phi]}{\partial \Phi} \tag{3.21}$$

with boundary conditions $x_0(0) = x_0$. To satisfy the above requirements, the possible choice of ϕ is $\phi = \Phi[t, x(t)]x$. In the multi-argument process, the similar choice of

the functional ϕ would be $\phi_i[t, x^i(t)] = \Phi_i(t)x^i(t)$. Using the formula of Eq. (3.7), the conditions can be rewritten into the form

$$\dot{\Phi} = -J^T(t)\Phi(t) + \frac{\partial f^0(t, x_0, c_0)}{\partial x}, \tag{3.22}$$

where

$$J_{ij} = \frac{\partial f^i(t, x_0, c_0)}{\partial x^j} \tag{3.23}$$

and $J^T(t)$ is the transpose matrix.

3.3.2 Second Order in x

If the equations of motion of the system are not linear, one need to consider an improvement form of ϕ. Since functional ϕ needs to satisfy Eq. (3.8) and Eq. (3.9), the simplest choice of functional ϕ is of the form

$$\begin{aligned}\phi(t, x(t)) &= \Phi_i(t)x^i + \frac{1}{2}\Sigma_{ij}(t)\Delta x^i \Delta x^j \quad (i, j = 1, 2, ..., n) \\ &\equiv \langle \Phi(t), x\rangle + \frac{1}{2}\langle \Delta x, \Sigma(t)\Delta x\rangle,\end{aligned} \tag{3.24}$$

where the $\Delta(x) \equiv x - x_0$ and both the vector-function $\phi(t)$ and the matrix $\Sigma(t)$ should be found. Here $\Sigma(t)$ is the matrix of the second derivatives of the function $\phi(t, x)$. The first necessary conditions for inequalities of Eq. (3.8) and Eq. (3.9) are equivalent to Eq. (3.19) and Eq. (3.20), and the second necessary conditions for inequalities of Eq. (3.8) and Eq. (3.9) yield the following differential inequalities:

$$d^2R \geq 0, \qquad d^2R = \left\langle \Delta x, \frac{\partial^2 R[t, x_0(t), c_0(t)]}{\partial x \partial x}\Delta x \right\rangle, \tag{3.25}$$

$$d^2G \leq 0, \qquad d^2G = \left\langle \Delta x, \frac{\partial^2 G[T, x_0(T)]}{\partial x \partial x}\Delta x \right\rangle. \tag{3.26}$$

For the reason that functional ϕ can be choose arbitrarily, one can require that the matrix $\Sigma(t)$ is a diagonal matrix and satisfy the above conditions, which means

$$\begin{aligned}\frac{\partial^2 R[t, x_0(t), c_0(t)]}{\partial x^i \partial x^j} &= 0, \quad i \neq j, \quad i, j = 1, 2, ..., n, \\ \frac{\partial^2 R[t, x_0(t), c_0(t)]}{\partial x^i \partial x^i} &= \Sigma_{ii}(t), \quad \Sigma_{ii}(t) \geq 0, \quad i = 1, 2, ..., n,\end{aligned} \tag{3.27}$$

and

$$\begin{aligned}\frac{\partial^2 G[T, x_0(T)]}{\partial x^i \partial x^j} &= 0, \quad i \neq j, \quad i, j = 1, 2, ..., n, \\ \frac{\partial^2 G[T, x_0(T)]}{\partial x^i \partial x^i} &= \Sigma_{ii}(T), \quad \Sigma_{ii}(T) \leq 0, \quad i = 1, 2, ..., n.\end{aligned} \tag{3.28}$$

One therefore can determine the equation of motion of $\Sigma(t)$ with boundary condition $\Sigma(T)$ by the above linear differential equation.

3.3.3 Algorithm

In previous section, Krotov's optimal method is already introduced and discussed in detail. Here we will summarize the algorithm for further extension.

(1) freely choose a history of control process $c_0(t)$.

(2) Use Eq. (3.1) and initial condition $x(0) = x_0$ to find the trajectory of $x_0(t)$.

(3) Find the functional $\Phi(t)$ by Eq. (3.17) and Eq. (3.18) or equivalently by Eq. (3.19) and Eq. (3.20).

(4) Use Eq. (3.27) and Eq. (3.28) to find the matrix $\Sigma(t)$.

(5) With the functional ϕ, the control $\tilde{c}(t)$ is found according to Eq. (3.10).

(6) Derive the new trajectory $x_1(t)$ and the new control control sequence $c_1(t)$ by Eq. (3.1).

(7) Repeat process (2) to (6) until the desired optimal value is achieved.

3.4 Examples

3.4.1 a Linear Problem

Consider a linear problem with ϕ chosen in the form in subsection (3.3.1) for the following optimal control problem. The function $x(t)$ and $c(t)$ are constructed by

$$\dot{x}(t) = i(1 + c(t))x(t), \quad x(0) = 1; \tag{3.29}$$

c(t) is real and one want to minimize the cost function

$$I = \mathrm{Re}[(1 - x(T)e^{i\pi})] + \frac{1}{2}b\int_0^T c^2(t')dt' \longrightarrow \min. \tag{3.30}$$

where $b > 0$.

Now we choose the parameters $b = 5$, $T = 2$ and substitute the linear form of $\phi = \Phi[t, x(t)]x$ bring into Eq. (3.3) and Eq. (3.4) to derive R and G :

$$R = \mathrm{Re}[\Phi(t)[i(1 + c(t))x(t)] + \frac{\partial}{\partial t}(\Phi(t)x(t))] - \frac{1}{2}bc^2(t), \tag{3.31}$$

$$G = \mathrm{Re}[(1 - x(T)e^{i\pi}) + \Phi(T)x(T)]. \tag{3.32}$$

Using Eq. (3.19) and Eq. (3.20), one can derive the equation of motion of Φ:

$$\dot{\Phi}(t) = i(1 + c(t))\Phi(t), \qquad \Phi(T) = e^{i\pi}. \tag{3.33}$$

Performing the algorithm described in subsection (3.3.3), we obtain the result shown in Fig. 3.1, where we have used the Runge Kutta method with the segment of integration partitioned into 200 intervals, and the fidelity is define as $\mathrm{Re}[x(T)e^{i\pi}]$. However, for a non-linear problem, the functional Φ will become more complex. Therefore we will discuss a simple non-linear problem in the next subsection.

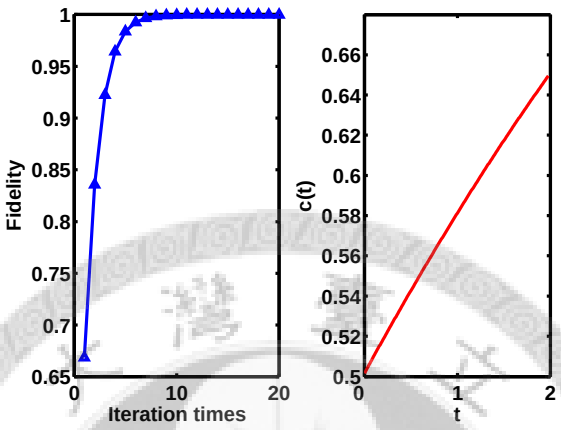

Figure 3.1: Left: fidelity versus iteration times. Right: optimal control sequences respect to time t.

3.4.2 a Non-Linear Problem

Let us consider the approach from subsection (3.3.2) for the following optimal control problem. The functions $x(t)$ and $c(t)$ are constructed by

$$\dot{x} = c, \quad |c| \leq 1, \quad x(0) = 0; \tag{3.34}$$

and one want to minimize the cost function

$$I = \int_0^T (c^2 - x^2)dt + \frac{1}{2}bx^2(T) \longrightarrow \min, \tag{3.35}$$

where $b > 0$.

Now we choose the parameters $b = 20$, $T = 4$ substitute Eq. (3.24) into Eq. (3.3) and Eq. (3.4) to derive R and G of the form

$$\begin{aligned} R &= \dot{\Phi}(t)x(t) + \frac{1}{2}\dot{\Sigma}(t)(\Delta x)^2 + \Phi(t)c(t) \\ &\quad +\Sigma\Delta x(t)(c(t) - c_0(t)) - c^2(t) + x^2(t), \qquad (3.36) \\ G &= \Phi(T)x(T) + \frac{1}{2}\Sigma(T)(\Delta x(T))^2 + \frac{1}{2}bx^2(T). \qquad (3.37) \end{aligned}$$

Since $R_{xx} = \dot{\Sigma}(t) + 1$ and $G_{xx} = \Sigma(T) + b$, we first choose that $\dot{\Sigma}(t) = 0$ and $\Sigma(T) = -b - 4$. Performing the algorithm described on subsection (3.3.3), we obtain

the result shown in Fig. 3.2, where we have use the Runge Kutta method with the segment of integration partitioned into 200 intervals. For comparison, the known solution of the problem is shown below

$$x(t) = \begin{cases} \pm t, & t \leq \tau_1, \\ \pm k\cos(t - T/2), & \tau_1 \leq t \leq \tau_2, \\ \pm T \mp t, & \tau_2 \leq t, \end{cases} \tag{3.38}$$

where T is the final time and τ_1, τ_2 and k are chosen according to smoothness conditions: $\dot{x} = \pm 1$ for $t = \tau_1$, $\dot{x} = \mp 1$ for $t = \tau_2$, $\pm t = \pm k\cos(t - T/2)$ at $t = \tau_1$ and $\pm k\cos(t - T/2) = \pm T \mp t$ at $t = \tau_2$. Note that the result of Krotov optimal method in Fig. 3.2 is equal to the known solution. Therefore the validity and usefulness of the Krotov optimal method are demonstrated. We will extend the Krotov optimal method to investigate quantum gate of closed quantum system in the next example.

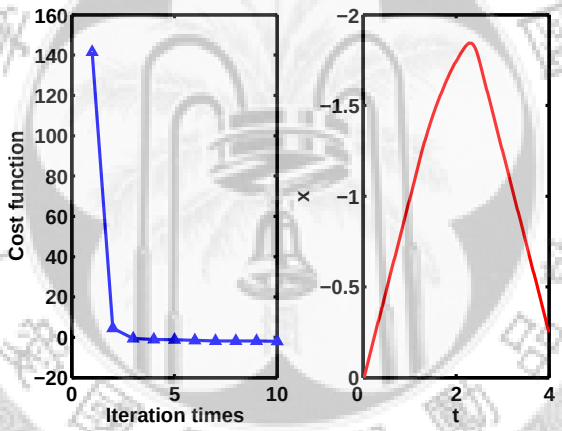

Figure 3.2: Left: Cost function versus iteration times. Right: Optimal evolution of x respect to time t.

3.4.3 The Closed Quantum System Problem

The time dependent Schrödinger equation for the evolution operator (propagator) $U(t)$ of a quantum system in an extended time-dependent control Hamiltonian $\mu\varepsilon(t)$ when the control parameters $\varepsilon(t)$ is read, can be written as

$$i\hbar \frac{\partial}{\partial t} U(t) \quad = \quad (H + \mu\varepsilon(t))U(t). \tag{3.39}$$

Suppose that one want to minimize the cost function

$$I \quad = \quad 1 - \mathrm{Re}[\mathtt{Tr}\{O^{\dagger}U(T)\}] + \lambda \int_0^T (\varepsilon(t') - \varepsilon_0)^2 dt' \longrightarrow \min. \tag{3.40}$$

where $\lambda > 0$ and ε_0 is an initial energy that can be considered as the restriction for the optimal control sequences; furthermore, ε_0 can also be time-dependent. O is a target goal for the propagator $U(T)$.

Now we choose the parameters $\lambda = 1$, $T = 1$ and substitute $\phi = B(t)U(t)$ into Eq. (3.3) and Eq. (3.4) to derive R and G :

$$R = \mathrm{Re}\left[\mathrm{Tr}\{B(t)(H+\mu\varepsilon(t))U(t) + \frac{\partial B(t)}{\partial t}U(t)\}\right] - \lambda(\varepsilon(t') - \varepsilon_0)^2, \quad (3.41)$$

$$G = \mathrm{Re}\left[\mathrm{Tr}\{O^\dagger U(T) - (B(t) - U(T))\,\big|_0^T\}\right]. \quad (3.42)$$

Using Eq. (3.19) and Eq. (3.20), one can derive the equation of motion of $B(t)$:

$$i\hbar\frac{\partial}{\partial t}B(t) = B(t)(H+\mu\varepsilon(t)), \qquad B(T) = O^\dagger. \quad (3.43)$$

Here we find out a straight way to derive optimal control sequences for every time interval by differential the function R respect to ε. Since the control value is chosen for a better result, we need to require $\partial R/\partial\varepsilon = 0$ and $\partial^2 R/(\partial\varepsilon)^2 \leq 0$. Therefore the optimal control sequences is of the form

$$\varepsilon(t) = \varepsilon_0 + \frac{1}{2\lambda}\mathrm{Re}[\mathrm{Tr}\{B(t)\mu U(t)\}]. \quad (3.44)$$

Using the algorithm in subsection (3.3.3) carefully with the above conditions where $B(t)$ depends on old $\varepsilon(t)$, and $U(t)$ is built from new $\varepsilon(t)$. Note that for a better performance, one can substitute ε_0 with old $\varepsilon(t)$ to derive new $\varepsilon(t)$. The system under consideration is a charge qubit built by Cooper pair box. Under appropriate conditions mentioned in 2.3.1 (chage energy E_C much larger than the Josephson coupling E_J and temperatures $k_B T \ll E_J$) only two charge states are important, and the Hamiltonian of the qubit reads

$$H(t) = -\varepsilon(t)\sigma_z/2 - \Omega\sigma_x/2 \quad (3.45)$$

where $H = \Omega\sigma_x/2$ and $\mu = \sigma_z/2$ and Ω is a bias voltage. If we consider a target goal

$$O = \begin{pmatrix} 1 & 0 \\ 0 & -1 \end{pmatrix}, \quad (3.46)$$

we obtain the result shown in Fig. 3.3, where we use the Euler method with the segment of integration partitioned into 100 intervals ($dt = 0.01T$), and fidelity is define as $\mathrm{Re}[\mathtt{Tr}\{O^\dagger U(T)\}]$. Note that this is a quantum optimal control problem of a single-qubit Z-gate and can be considered as the fundamental quantum computation problem of optimal control.

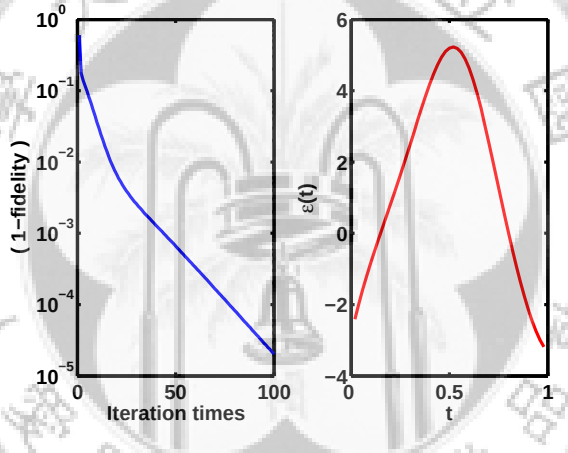

Figure 3.3: Left: (1-fidelity) versus iteration times. Right: optimal control sequence as a function of time t.

Chapter 4

Open Quantum System

4.1 Master Equation

4.1.1 Density Matrix

For a closed quantum system, the physical object obeys Schrödinger equation,

$$\frac{\partial}{\partial t}|\psi\rangle = -\frac{i}{\hbar}H|\psi\rangle, \tag{4.1}$$

where H is the total Hamiltonian. The density matrix can be defined as $\rho = |\psi\rangle\langle\psi|$. Using Schrödinger equation Eq. (4.1), we can get the equation of motion of the density matrix $\dot{\rho}$,

$$\begin{aligned}
\dot{\rho} &= (|\dot{\psi}\rangle\langle\psi| + |\psi\rangle\langle\dot{\psi}|) \\
&= (-\frac{i}{\hbar}H|\psi\rangle\langle\psi| + \frac{i}{\hbar}|\psi\rangle\langle\psi|H) \\
&= -\frac{i}{\hbar}(H|\psi\rangle\langle\psi| - |\psi\rangle\langle\psi|H) \\
&= -\frac{i}{\hbar}(H\rho - \rho H) \\
&= -\frac{i}{\hbar}[H,\rho],
\end{aligned} \tag{4.2}$$

Equation (4.2) is called Liouville-Von Neumann equation of motion for density matrix. Note that Liouville equation, Eq. (4.2), can only be used in closed quantum system. Hence, it is not valid for the subsystem of a composite system whose subsystems have interaction with each other. The equation can only describe the whole system, including the subsystem in which we are interested, and the rest of the system. The next section, we will discuss how to write down the equation of motion for the subsystem in which we are interested.

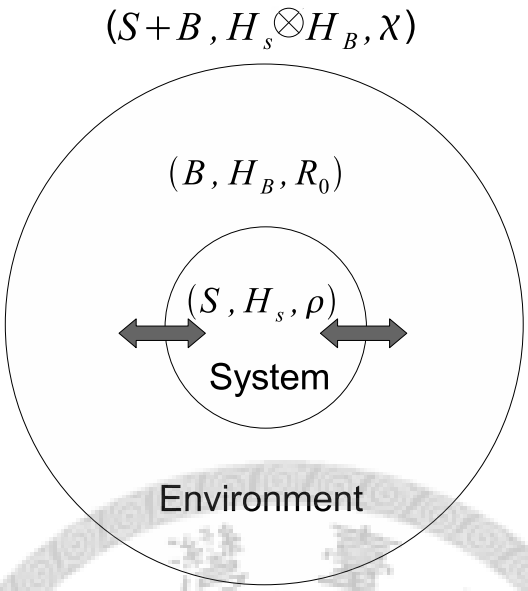

Figure 4.1: Schematic picture of an open system

4.1.2 The Derivation

Because that Eq. (4.2) can only be used in a closed system, when we solve a composite system, we can divide the system into two parts. A schematic picture is shown in Fig. 4.1 One part is the subsystem in which we are interested, and the other is called a bath. The Hamiltonian of the subsystem is time dependent, $H_S(t)$, and the bath is the rest system with Hamiltonian, H_B. Also, consider that the subsystem and bath couple to each other, and the interaction Hamiltonian of the coupling term is noted as H_{SB}. Hence, the total Hamiltonian can be written as,

$$H(t) = H_S(t) \otimes I_B + I_S \otimes H_B + H_{SB}, \tag{4.3}$$

and the Hilbert space of the total system is defined by a tensor product,

$$\mathcal{H} = \mathcal{H}_\mathcal{S} \otimes \mathcal{H}_\mathcal{B}. \tag{4.4}$$

Define the total density matrix (subsystem and bath) as $\chi(t)$ obeying Liouville-Von Neumann equation (4.2),

$$\dot{\chi}(t) = -\frac{i}{\hbar}[H(t), \chi(t)], \tag{4.5}$$

where $H(t)$ is given by Eq. (4.3). In general, we usually assume that the interaction Hamiltonian between the subsystem and bath is very weak compared with the rest of the Hamiltonian. Therefore, we may use the interaction picture that fix the dominate

Hamiltonian term, the subsystem and bath Hamiltonian, $H_S + H_B$. Define that

$$\begin{aligned}\tilde{\chi}(t) &= e^{\frac{i}{\hbar}(H_S+H_B)t}\chi(t)e^{-\frac{i}{\hbar}(H_S+H_B)t},\\ \chi(t) &= e^{-\frac{i}{\hbar}(H_S+H_B)t}\tilde{\chi}(t)e^{\frac{i}{\hbar}(H_S+H_B)t},\end{aligned} \tag{4.6}$$

and differential Eq. (4.6) with respect to time

$$\begin{aligned}\dot{\chi}(t) &= -\frac{i}{\hbar}(H_S+H_B)e^{-\frac{i}{\hbar}(H_S+H_B)t}\tilde{\chi}(t)e^{\frac{i}{\hbar}(H_S+H_B)t}\\ &\quad +e^{-\frac{i}{\hbar}(H_S+H_B)t}\dot{\tilde{\chi}}(t)e^{\frac{i}{\hbar}(H_S+H_B)t}\\ &\quad +\frac{i}{\hbar}e^{-\frac{i}{\hbar}(H_S+H_B)t}\tilde{\chi}(t)(H_S+H_B)e^{\frac{i}{\hbar}(H_S+H_B)t}.\end{aligned} \tag{4.7}$$

Then using Eq. (4.5), we obtain

$$\begin{aligned}\dot{\chi}(t) &= -\frac{i}{\hbar}[H_S+H_B+H_{SB},\chi(t)]\\ &= -\frac{i}{\hbar}(H_S+H_B+H_{SB})e^{-\frac{i}{\hbar}(H_S+H_B)t}\tilde{\chi}(t)e^{\frac{i}{\hbar}(H_S+H_B)t}\\ &\quad +\frac{i}{\hbar}e^{-\frac{i}{\hbar}(H_S+H_B)t}\tilde{\chi}(t)e^{\frac{i}{\hbar}(H_S+H_B)t}(H_S+H_B+H_{SB}).\end{aligned} \tag{4.8}$$

Comparing with Eq. (4.7) and Eq. (4.8), we can get

$$\begin{aligned}&e^{-\frac{i}{\hbar}(H_S+H_B)t}\dot{\tilde{\chi}}(t)e^{\frac{i}{\hbar}(H_S+H_B)t}\\ &\quad = -\frac{i}{\hbar}H_{SB}e^{-\frac{i}{\hbar}(H_S+H_B)t}\tilde{\chi}(t)e^{\frac{i}{\hbar}(H_S+H_B)t}\\ &\quad\quad +\frac{i}{\hbar}e^{-\frac{i}{\hbar}(H_S+H_B)t}\tilde{\chi}(t)e^{\frac{i}{\hbar}(H_S+H_B)t}H_{SB}.\end{aligned} \tag{4.9}$$

Defining

$$\tilde{H}_{SB}(t) = e^{\frac{i}{\hbar}(H_S+H_B)t}H_{SB}e^{-\frac{i}{\hbar}(H_S+H_B)t}, \tag{4.10}$$

and inserting the Eq. (4.10) into the Eq. (4.9), we obtain

$$\begin{aligned}\dot{\tilde{\chi}}(t) &= -\frac{i}{\hbar}e^{\frac{i}{\hbar}(H_S+H_B)t}H_{SB}e^{-\frac{i}{\hbar}(H_S+H_B)t}\tilde{\chi}(t)+\frac{i}{\hbar}\tilde{\chi}(t)e^{\frac{i}{\hbar}(H_S+H_B)t}H_{SB}e^{-\frac{i}{\hbar}(H_S+H_B)t}\\ &= -\frac{i}{\hbar}[\tilde{H}_{SB},\tilde{\chi}(t)].\end{aligned} \tag{4.11}$$

One may integrate Eq. (4.11) to obtain

$$\tilde{\chi}(t) = \tilde{\chi}(0) - \int_0^t \frac{i}{\hbar}[\tilde{H}_{SB}(t'),\tilde{\chi}(t')]dt'. \tag{4.12}$$

Taking Eq. (4.12) and inserting it back into Eq. (4.11), we can get

$$\begin{aligned}\dot{\tilde{\chi}}(t) &= -\frac{i}{\hbar}[\tilde{H}_{SB}(t),\tilde{\chi}(0)-\int_0^t\frac{i}{\hbar}[\tilde{H}_{SB}(t'),\tilde{\chi}(t')]dt']\\ &= -\frac{i}{\hbar}[\tilde{H}_{SB}(t),\tilde{\chi}(0)]-\frac{1}{\hbar^2}\int_0^t[\tilde{H}_{SB}(t),[\tilde{H}_{SB}(t'),\tilde{\chi}(t')]].\end{aligned} \tag{4.13}$$

However, we are just interested in the evolution of the subsystem. Hence, we can define the reduced density matrix of the subsystem as ρ satisfying that

$$\rho(t) = \mathrm{Tr}_{\mathrm{Bath}}[\chi(t)] = \mathrm{Tr}_B[\chi(t)] \tag{4.14}$$

If we take the trace of the full density matrix over the bath, in the interaction picture, we can get

$$\begin{aligned}
Tr_B[\tilde{\chi}(t)] &= Tr_B[e^{\frac{i}{\hbar}(H_S+H_B)t}\chi(t)e^{-\frac{i}{\hbar}(H_S+H_B)t}] \\
&= e^{\frac{i}{\hbar}H_St}Tr_B[e^{\frac{i}{\hbar}H_Bt}\chi(t)e^{-\frac{i}{\hbar}H_Bt}]e^{-\frac{i}{\hbar}H_St} \\
&= e^{\frac{i}{\hbar}H_St}[\sum_i \langle\phi_i^B|e^{\frac{i}{\hbar}H_Bt}\chi(t)e^{-\frac{i}{\hbar}H_Bt}|\phi_i^B\rangle]e^{-\frac{i}{\hbar}H_St} \\
&= e^{\frac{i}{\hbar}H_St}[\sum_i \langle\phi_i^B|e^{\frac{i}{\hbar}E_i^Bt}\chi(t)e^{-\frac{i}{\hbar}E_i^Bt}|\phi_i^B\rangle]e^{-\frac{i}{\hbar}H_St} \\
&= e^{\frac{i}{\hbar}H_St}[\sum_i \langle\phi_i^B|\chi(t)|\phi_i^B\rangle]e^{-\frac{i}{\hbar}H_St} \\
&= e^{\frac{i}{\hbar}H_St}Tr_B[\chi(t)]e^{-\frac{i}{\hbar}H_St} \\
&= e^{\frac{i}{\hbar}H_St}\rho e^{-\frac{i}{\hbar}H_St} \\
&= \tilde{\rho}(t),
\end{aligned} \tag{4.15}$$

where E_i^B and $|\phi_i^B\rangle$ correspond to the eigenvalues and eigenstates of H_B. In the interaction picture, the density matrix of the subsystem is related to ρ in the Schrödinger pictures

$$\tilde{\rho}(t) = e^{\frac{i}{\hbar}H_St}\rho e^{-\frac{i}{\hbar}H_St}. \tag{4.16}$$

It means that the transformation between ρ and $\tilde{\rho}$ depends only on the Hamiltonian of the subsystem H_S. Using Eq. (4.13) and the Eq. (4.15), we can get

$$\begin{aligned}
\dot{\tilde{\rho}}(t) &= \frac{\partial}{\partial t}Tr_B[\tilde{\chi}(t)] = Tr_B[\dot{\tilde{\chi}}(t)] \\
&= -\frac{i}{\hbar}[\tilde{H}_{SB}(t), \tilde{\chi}(0)] - \frac{1}{\hbar^2}\int_0^t [\tilde{H}_{SB}(t), [\tilde{H}_{SB}(t'), \tilde{\rho}(t')]]dt'.
\end{aligned} \tag{4.17}$$

Equation (4.17) is still exact but is difficult to solve in general. In the next two sections, we will introduce two approximations, the Born approximation and the Markovian approximation, to Eq. (4.17).

4.1.3 Born Approximation

In Born approximation, we will assume that there the interaction is turned on at $t = 0$ and that no correlations exist between S and R at this initial time. Then $\chi(0) = \tilde{\chi}(0)$ factorizes as

$$\chi(0) = \rho(0) \otimes R_0, \tag{4.18}$$

where R_0 is an initial reservoir density matrix of the bath. Then noting that

$$\mathrm{Tr}[\tilde{\chi}(t)] = e^{(i/hbar)H_s t}\rho(t)e^{-(i/hbar)H_s t} \equiv \tilde{\rho}(t), \tag{4.19}$$

after tracing over the reservoir, eq. (4.17) gives the master equation

$$\dot{\tilde{\rho}} = -\frac{1}{\hbar^2}\int_0^t dt' \mathrm{Tr}_R\{[\tilde{H}_{SR}(t), [\tilde{H}_{SR}(t'), \tilde{\chi}(t')]]\}, \tag{4.20}$$

where, for simplicity, we have eliminated the term $(1/i\hbar)\mathrm{Tr}_R\{[\tilde{H}_{SR}(t), \chi(0)]\}$ with the assumption

$$\mathrm{Tr}_R[\tilde{H}_{SR}(t)R_0] = 0. \tag{4.21}$$

This is guaranteed if the reservoir operators coupling to S have zero mean in the state R_0. The environment or reservoir by definition is large and contains many degrees of freedom so that the influence of the system on the reservoir is small in the weak system–environment coupling case. As a consequence, to second order in system–environment interaction, the total density operator on the right-hand side of Eq. (4.20) can be approximated to an uncorrelated (factorized) state as

$$\tilde{\chi}(t) = \tilde{\rho}(t) \otimes R_0 + O(H_{SB}). \tag{4.22}$$

since the products of two interaction Hamiltonians H_I's appear already there. So in many textbooks, the replacement of

$$\tilde{\chi}(t') = \tilde{\rho}(t') \otimes R_0 \tag{4.23}$$

is performed under the so-called Born approximation. One then obtains

$$\dot{\tilde{\rho}}(t) \;=\; -\frac{1}{\hbar^2}\int_0^t \mathrm{Tr}_B[\tilde{H}_{SB}(t), [\tilde{H}_{SB}(t'), \tilde{\rho}(t') \otimes R_0]]dt'. \tag{4.24}$$

In general, we usually assume that the density matrix of the bath stays in thermal equilibrium as the form

$$R_0 = \frac{e^{-\beta H_B}}{Tre^{-\beta(H_B)}}. \tag{4.25}$$

However, the Eq. (4.24) is the time-nonlocal (or time-convolution) formula, and the equation of motion could be very complicated. That is because of the future evolution $\tilde{\rho}(t)$ depends on its past history through the integral over $\tilde{\rho}(t')$. It can also be shown that another systematically perturbative non-Markovian master equation that is local in time can be derived from the time-convolutionless projection operator formalism. Under the similar assumption of the factorized initial system–reservoir density matrix state, the second-order time-convolutionless master equation in the interaction picture can be obtained as

$$\dot{\tilde{\rho}}(t) \;=\; -\frac{1}{\hbar^2}\int_0^t \mathrm{Tr}_B[\tilde{H}_{SB}(t), [\tilde{H}_{SB}(t'), \tilde{\rho}(t) \otimes R_0]]dt'. \tag{4.26}$$

We note here that obtaining the time-convolutionless non-Markovian master equation perturbatively up to only second order in the interaction Hamiltonian using the time-convolutionless projection operator technique is equivalent to obtaining it by replacing $\rho(\tilde{t'})$ with $\rho(\tilde{t})$ in Eq. (4.24).

4.1.4 Markov Approximation

In a large bath maintained in thermal equilibrium, the environment may be not possible memorizing the influence of the system and reflect it back for very long; not for long enough to significantly affect the future evolution of S. Therefore, with the view in mind we can make the underlying assumption of the Markov approximation more explicit.

Let us consider a more specific form of coupling interaction H_{SB} can be written as

$$H_{SB} = \sum_j S_j \otimes B_j, \tag{4.27}$$

where S_j are the system operators in the Hilbert space of S and B_j are the bath operators, operators in the Hilbert space of R. Then

$$\begin{aligned}
\tilde{H}_{SR}(t) &= \sum_j e^{(i/\hbar)(H_S+H_R)t} S_j \otimes B_j e^{-(i/\hbar)(H_S+H_R)t} \\
&= \sum_j (e^{(i/\hbar)H_S t} S_j e^{-(i/\hbar)H_S t}) \otimes (e^{(i/\hbar)H_B t} B_j e^{-(i/\hbar)H_B t}) \\
&= \sum_j \tilde{S}_j \otimes \tilde{B}_j.
\end{aligned} \tag{4.28}$$

Inserting Eq. (4.28) into Eq. (4.24),

$$\begin{aligned}
\dot{\tilde{\rho}}(t) &= -\frac{1}{\hbar^2} \int_0^t \sum_{j,k} \mathrm{Tr}_B[\tilde{S}_j \otimes \tilde{B}_j, [\tilde{S}_k \otimes \tilde{B}_k, \tilde{\rho}(t') \otimes R_0]] dt' \\
&= -\sum_{j,k} \int_0^\infty \mathrm{Tr}_B[\tilde{S}_j(t)\tilde{B}_j(t), [\tilde{S}_k(t')\tilde{B}_k(t'), \tilde{\rho}(t') \otimes R_0]] dt', \\
&= -\sum_{j,k} \int_0^\infty ((\tilde{S}_j(t)\tilde{S}_k(t')\tilde{\rho}(t') - \tilde{S}_k(t')\tilde{\rho}(t')\tilde{S}_j(t))\langle \tilde{B}_j(t)\tilde{B}_k(t')\rangle_R \\
&\quad + [\tilde{\rho}(t')\tilde{S}_k(t')\tilde{S}_j(t) - \tilde{S}_j\tilde{\rho}(t')\tilde{S}_k(t')]\langle \tilde{B}_k(t')\tilde{B}_j(t)\rangle_R) dt',
\end{aligned} \tag{4.29}$$

where we have used cyclic property of the trace and define that

$$\langle \tilde{B}_j(t)\tilde{B}_k(t')\rangle_R = Tr[R_0 \tilde{B}_j(t)\tilde{B}_k(t')], \tag{4.30}$$

$$\langle \tilde{B}_k(t')\tilde{B}_j(t)\rangle_R = Tr[R_0 \tilde{B}_k(t')\tilde{B}_j(t)]. \tag{4.31}$$

We further define the above formula called the bath correlation function

$$C_{jk}(t-t') \equiv Tr_B[\tilde{B}_j(t)\tilde{B}_k(t')R_0]. \tag{4.32}$$

We can justify the replacement of $\tilde{\rho}(t')$ by $\tilde{\rho}(t)$ and the integral upper bound $t \to \infty$ if these correlation functions decay very rapidly on the timescale on which $\tilde{\rho}(t)$ varies. Ideally, we might take

$$C_{jk} \propto \delta(t - t'). \tag{4.33}$$

The Markov approximation then relies on the existence of two widely separated time scales: a relatively small time scale for the dynamics of the system S, and a fast time scale characterizing the decay of reservoir correlation functions.

4.2 Master Equation of a Time-Dependent Non-Markovian spin-boson model

4.2.1 Model

We use the computational basis $\{|1\rangle, |2\rangle\}$ to describe a charge qubit system S (mentioned in 2.3.1) embedded in a dissipative environment B and interacting with a time-dependent control field. The total Hamiltonian is given by $H = H_S(t) + H_{SB} + H_B$. The Hamiltonian $H_S(t)$ is written as

$$H_S(t) = -\varepsilon(t)\sigma_z/2 - \Omega\sigma_x/2, \tag{4.34}$$

here Ω is the tunneling splitting and $\varepsilon(t)$ is the control field. In the notation of the second quantization, H_B takes the form

$$H_B = \sum_q \hbar\omega_q {b_q}^\dagger b_q, \tag{4.35}$$

${b_q}^\dagger$ and b_q are creation and annihilation of the bath oscillator mode q with frequency ω_q, respectively. The interaction Hamiltonian H_{SB} between the system and the environment is of the form

$$H_{SB} = \sigma_x \sum_q c_q (b_q + {b_q}^\dagger)/2. \tag{4.36}$$

where c_q is the coupling constant of mode q.

4.2.2 Derivation of the quantum Master Equation

In order to investigate dissipation and decoherence in an open quantum system, the density matrix formalism can be used to derive a master equation for the case of a subsystem

interacting with an environment. First, rotating the Hamiltonian to the interaction picture:

$$\begin{aligned}
\tilde{H}_{SB}(t) &= (T_- e^{\frac{i}{\hbar}\int_0^t (H_S(t')+H_B)dt'}) H_{SB} (T_+ e^{-\frac{i}{\hbar}\int_0^t (H_S(t')+H_B)dt'}) \\
&= (T_- e^{\frac{i}{\hbar}\int_0^t H_S(t')dt'})(e^{\frac{i}{\hbar}H_B t} H_{SB} e^{-\frac{i}{\hbar}H_B t})(T_+ e^{-\frac{i}{\hbar}\int_0^t H_S(t')dt'}) \\
&= (T_- e^{\frac{i}{\hbar}\int_0^t H_S(t')dt'})[\sigma_x(\sum_q c_q b_q e^{-i\omega_q t} + c_q b_q^\dagger e^{i\omega_q t})](T_+ e^{-\frac{i}{\hbar}\int_0^t H_S(t')dt'}) \\
&= (U(t)\sigma_x U^\dagger(t))B(t) \\
&= \tilde{\sigma}_x(t) B(t), \qquad (4.37)
\end{aligned}$$

where $U(t) = T_- e^{\frac{i}{\hbar}\int_0^t H_S(t')dt'}$, T_- means time-ordering in negative direction and $B(t) = \sum_q c_q b_q e^{-i\omega_q t} + c_q b_q^\dagger e^{i\omega_q t}$. Substituting into Eq. (4.24), one can derive

$$\begin{aligned}
\dot{\tilde{\rho}}(t) &= -\frac{1}{\hbar^2}\int_0^t Tr_B[\tilde{\sigma}_x(t)B(t), [\tilde{\sigma}_x(t')B(t'), \tilde{\rho}(t')\otimes R_0]]dt' \\
&= -\frac{1}{\hbar^2}\int_0^t dt' \left[(\tilde{\sigma}_x(t)\tilde{\sigma}_x(t')\tilde{\rho}(t') - \tilde{\sigma}_x(t)\tilde{\rho}(t')\tilde{\sigma}_x(t'))Tr_B[B(t)B(t')R_0]\right. \\
&\quad \left. + (\tilde{\rho}(t')\tilde{\sigma}_x(t')\tilde{\sigma}_x(t) - \tilde{\sigma}_x(t)\tilde{\rho}(t')\tilde{\sigma}_x(t'))Tr_B[B(t')B(t)R_0]\right], \qquad (4.38)
\end{aligned}$$

Rotating back to the Schrödinger picture, we can derive the equation of motion of the form

$$\dot{\rho}(t) = -\frac{i}{\hbar}[H_S(t), \rho(t)] + \{[\sigma_x, \mathcal{D}(t)] + [\mathcal{D}^\dagger(t), \sigma_x]\}, \qquad (4.39)$$

where $\mathcal{D}(t) = \frac{1}{(i\hbar)^2} U^\dagger(t)\int_0^t U(t')\sigma_x U^\dagger(t') Tr_B[B(t)B(t')R_0]dt' U(t)$. In the following, we define the bath correlation function $C(t-t') \equiv Tr_B[B(t)B(t')R_0]$. It can be evaluated as

$$\begin{aligned}
C(t-t') &= Tr_B\left[(\sum_q c_q b_q e^{-i\omega_q t} + c_q b_q^\dagger e^{i\omega_q t})(\sum_{q'} c_{q'} b_{q'} e^{-i\omega_{q'} t'} + c_{q'} b_{q'}^\dagger e^{i\omega_{q'} t'})R_0\right] \\
&= \sum_q |c_q|^2 \left(Tr_B[b_q b_q^\dagger R_0]e^{-i\omega_q(t-t')} + Tr_B[b_q^\dagger b_q R_0])e^{i\omega_q(t-t')}\right) \\
&= \int_0^\infty d\omega J(\omega)[(n(\omega)+1)e^{-i\omega(t-t')} + n(\omega)e^{i\omega(t-t')}] \qquad (4.40)
\end{aligned}$$

where $J(\omega) = \sum_q |c_q|^2 \delta(\omega - \omega_q)$ is the spectral density and $n(\omega)$ is the canonical ensemble average occupation number of the bath. Note that we convert $|c_q|^2 \mathrm{Tr}_B[b_q^\dagger b_q R_0]$ to $J(\omega_q)n(\omega_q)$ and treat $\omega_q \to \omega$ in the continuum limit.

4.3 Superoperator and Column Vector

In open quantum system problems, one usually uses superoperators to simplify the notation and for numerical calculation one also has to consider the density matrix as a column

vector to reduce difficulty. To illustrate what we mean, we first consider the case that the density matrix ρ of a quantum system has $N \times N$ dimensions. The equation of motion of the density matrix can be written as

$$\begin{aligned} \dot{\rho}(t) &= -\frac{i}{\hbar}[H_S, \rho], \\ &= \mathcal{L}_s[\rho], \end{aligned} \tag{4.41}$$

where H_S is full Hamiltonian of the system, and the $\mathcal{L}_s$ is Liouville superoperator. Now if we transform the density matrix into a column vector, the relation for operator and density matrix is

$$A\rho B = A \begin{pmatrix} \rho_{11} & \rho_{12} & \cdots & \rho_{1n} \\ \rho_{21} & \rho_{22} & \cdots & \rho_{2n} \\ \vdots & \vdots & \ddots & \vdots \\ \rho_{n1} & \rho_{n2} & \cdots & \rho_{nn} \end{pmatrix} B \Longrightarrow A \otimes B^T \begin{pmatrix} \rho_{11} \\ \rho_{12} \\ \vdots \\ \rho_{1n} \\ \rho_{21} \\ \vdots \\ \rho_{nn} \end{pmatrix}. \tag{4.42}$$

Therefore, we denote ρ^c as the transformed of density matrix in the column vector form that has $1 \times N^2$ dimensions and denote $\mathcal{L}_s^c$ as the corresponding superoperator to ρ^c.

Equation (4.41) is the equation of motion for the state density matrix. But for quantum gate operations we want to obtain the equation of motion for operator evolution, so we use the Eq.(4.41) and the relation $\rho(t) = U(t)\rho(0)U^\dagger(t) = \mathcal{U}(t)\rho(0)$, where $\mathcal{U}(t) = T_+\exp\{\int_0^t d\tau \mathcal{L}_s(\tau)\}$ is the propagator in superoperator form and $U(t) = T_+\exp\{\int_0^t d\tau - iH_s(\tau)\}$ is the propagator. We can use above to derive

$$\begin{aligned} \frac{d}{dt}(\mathcal{U}(t)\rho(0)) &= \mathcal{L}_s(t)\mathcal{U}(t)\rho(0), \\ \dot{\mathcal{U}}(t)\rho(0) &= \mathcal{L}_s(t)\mathcal{U}(t)\rho(0), \\ \Rightarrow \dot{\mathcal{U}}(t) &= \mathcal{L}_s(t)\mathcal{U}(t). \end{aligned} \tag{4.43}$$

For numerical calculation, the same equation in the column vector form is much easier to important. That is

$$\dot{\mathcal{U}}^c(t) = \mathcal{L}_s^c(t)\mathcal{U}^c(t). \tag{4.44}$$

Chapter 5

Optimal Control for One Qubit Quantum Gate

5.1 Introduction

One of the fundamental criteria for physical implementation of a practical quantum computer is to design a reliable universal set of quantum gates. A promising class of candidates for realization of scalable quantum computers are solid-state quantum devices based on superconducting Josephson-junction qubits. Series of beautiful experiments (charge, flux, phase) have been demonstrated and theoretical proposals related to Josephson-junction qubits have been investigated [33, 29, 21, 23, 30, 24, 28]. Typically, a central challenge to overcome in this enterprise is decoherence and dissipation induced by the coupling to the surrounding environment. Therefore it is important to find strategies to alleviate the problems and to build quantum gates operation for the purpose of quantum information processing. Optimal control method is one of the powerful tools already applied to the problem of dynamical decoupling from the environment and to finding the control sequence for high-fidelity quantum gates. It has also been extended to treat quantum systems with noise, imperfections and leakage to noncomputational states [16, 30, 25]. Furthermore, optimal control technique has recently been applied to Markovian open quantum systems in which the approximation of the bath correlation function being delta-correlated in time is assumed [22]. However, in some real experiments, we need to consider the non-local memory effects of the bath on the dynamics of the qubits. Especially, the bath memory effects are typically non-negligible in solid state devices. Thus it is desirable to apply optimal control technique to quantum gate operations in the non-Markovian open quantum systems [6, 29, 20, 4, 7, 8]. Some experiment related to controlling an open quantum system have also been demonstrated [1, 17] and open the possibilities to the optimal control in an open quantum system.

In this chapter we apply the optimal control method based on Krotov's method [26, 18, 19, 10, 32, 14] to a Non-Markovian quantum system. The optimal control method is developed based on a quantum dissipation formulation that treats the effect of dissipative terms in the equation of motion as many auxiliary subsystem density matrices coupled to the original density matrix of the qubits system [15, 32]. The state-independent super-operator formulation of optimal control is implemented. Finally, we apply the optimal control method to a single qubit gate embedded in a non-Markovian bosonic bath with ohmic spectrum. We show that under specific conditions, optimal control method can considerably reduce error from the non-Markovian bath and give a high fidelity Z-gate.

5.2 Quantum Dynamics

The spin-boson model is a widely used and thoroughly investigated systems to describe dissipation and decoherence in open quantum systems, especially for modelling qubit systems for quantum computation purposes. Here we use this model to describe super-conducting charge qubit interacting with a non-Makrovian environment. We apply the time-nonlocal or time-convolution master equation whereby the dissipator is computed within second order in the spin-boson interaction to find the optimal control sequence.

5.2.1 Model

We use the computational basis $\{|1\rangle, |2\rangle\}$ to describe a qubit system S embedded in a dissipative environment B and subject to a time-dependent control field. The total Hamiltonian is given by $H = H_S(t) + H_I + H_B$. The Hamiltonian $H_S(t)$ is written as

$$H_S(t) = -\varepsilon(t)\sigma_z/2 - \Omega\sigma_x/2, \tag{5.1}$$

here Ω is the tunneling splitting and $\varepsilon(t)$ is the control pulse. H_B and H_I are described in section 4.2.

In order to investigate dissipation and decoherence in open quantum systems, the density matrix formalism can be used to derive a master equation for the case a subsystem interacting with an environment from Eq. (4.39), we obtain [2, 5, 29]

$$\dot{\rho}(t) = \mathcal{L}_s(t)\rho(t) + [\mathcal{L}_x\mathcal{D}(t) + \{H.C.\}], \tag{5.2}$$

where $\mathcal{L}_S(t) = \frac{1}{i\hbar}[H_S(t), \bullet]$ and $\mathcal{L}_x = \frac{1}{i\hbar}[\sigma_x, \bullet]$. The dissipation operators can be written as [11]

$$\mathcal{D}(t) = \frac{1}{i\hbar}\int_0^t dt' \mathcal{U}_S(t,t')\sigma_x C(t-t')\rho(t'), \tag{5.3}$$

where the propagator superoperator $\mathcal{U}_S(t,t') = T_+ exp\{\int_{t'}^{t} d\tau \mathcal{L}_S(\tau)\}$ and the bath correlation function can be written as

$$\begin{aligned} C(t-t') &= \frac{1}{2\pi}\int_0^\infty d\omega J(\omega)\cos(\omega(t-t'))\coth(\frac{\beta\omega}{2}) \\ &\quad -\frac{i}{2\pi}\int_0^\infty d\omega J(\omega)\sin(\omega(t-t')), \end{aligned} \tag{5.4}$$

with $\beta \equiv 1/T$ ($k_B = 1$), taking into account all the effects of the bosonic bath. We take the ohmic spectral density

$$J(\omega) = 2\pi\alpha\omega e^{-\omega/\omega_c}, \tag{5.5}$$

where α is a dimensionless coupling constant, and where ω_c is the bath cutoff frequency. The result of the bath correlation function from Eq. (5.4) can be calculated in an analytic form of

$$C(t-t') = \frac{\alpha\omega_c^2}{[i+\omega_c(t-t')]^2} + \frac{2\alpha}{\beta^2} Re\left[\psi'\left(\frac{1+i\omega_c(t-t')}{\beta\omega_c}\right)\right]. \tag{5.6}$$

Here $\psi'(z)$ is the derivative of the digamma function [29]. We note that

$$C(t-t') = C^*(t'-t). \tag{5.7}$$

The dissipator defined in Eq. (5.3) contains the bath correlation function and the time-ordered system propagator superoperator $\mathcal{U}_s(t,t')$ that involves the control field through $H_S(t)$ in $\mathcal{L}_s(t)$. Thus the control field and dissipation are correlated. This paves the way to manipulate the control field to counteract the effect of the environment on the system dynamics. However, the time-convolution master equation, Eq. (5.2), togather with the dissipator $\mathcal{D}(t)$ defined in Eq. (5.3) is a time-ordered integro-differential equation for non-commuting system and control operators. Is is thus difficult to solve. It is possible to transform it into a time-local differential equations. The price to pay is to introduce auxiliary density matrices with a extended Liouville space. We describe the procedure to achieve this in the master equation in the next section.

5.2.2 Equation of motion in the extended Liuville space

To cope with the time-convolution non-Markovian quantum master equation, Meier and Tannor [15] proposed a bath spectral density parametrization method to properly the bath express correlation functions in a multi-exponential form. This work was further approached by Xu and Yan [31] to construct an improved quantum dynamics theory named CS-QDT (complete second-order quantum dissipation theory), in which the second-order correlated system-bath canonical state is used as the initial condition. Here we shall use a

similar algebraic approach to construct the equation of motion for the dissipators. Since we already know the integral form of the ohmic bath in Eq. (5.6), we will focus on the correlation function $\mathcal{C}(t-t')$ and expand it directly by exponential functions with the following form, instead of parametrizing the spectral density in a Lorentz form in the frequency domain first. The bath correlation function can then be expressed as

$$C(t-t') = \sum_j C_j(0) e^{\gamma_j (t-t')} = \sum_j C_j(t-t'), \tag{5.8}$$

where $C_j(0)$ and γ_j are complex constants and can be found by numerical method. Here we use the toolbox in MATLAB called `lsqcurvefit` to find the value of $C_j(0)$ and r_j. Therefore, the dissipation operators $\mathcal{D}(t)$ can be expanded with the form $\mathcal{D}(t) = \sum_j \mathcal{K}_j(t)$, where

$$\mathcal{K}_j(t) = \frac{1}{i\hbar} \int_0^t dt' \mathcal{U}_S(t-t') \sigma_x C_j(t-t') \rho(t'). \tag{5.9}$$

Note that Eq. (5.9) is still a time-nonlocal and time-ordered integration for non-commuting operators. Therefore, we use the auxiliary density matrix $\mathcal{K}_j(t)$ to replace $\mathcal{D}(t)$ and find the time derivative for $\mathcal{K}_j(t)$ is of the form

$$\dot{\mathcal{K}}_j(t) \;=\; \frac{1}{i\hbar} C_j(0) \sigma_x \rho(t) + (\mathcal{L}_S(t) + \gamma_j) \mathcal{K}_j(t), \tag{5.10}$$

The same process can be done for the Hermitian conjugate part $\mathcal{D}^\dagger(t) \equiv \sum_j {\mathcal{K}_j}^\dagger(t)$. The equation of motion is written as

$$\dot{{\mathcal{K}_j}}^\dagger(t) = \frac{1}{i\hbar} {C_j}^*(0) \rho(t) \sigma_x + {\mathcal{K}_j}^\dagger(t) (\mathcal{L}_S(t) + {\gamma_j}^*), \tag{5.11}$$

The Eq. (5.2) combining with Eq. (5.10) and Eq. (5.11) form a set of coupled linear equations of motion. Obviously, the above equations are time-local and have no time-ordering and integrating problems. One can has the extended equation of motions. The initial conditions for above set of coupled equations of motion are $\rho(0) = \rho_0$ and $\mathcal{K}_j(0) = 0$.

5.2.3 State-independent superoperator formulation in the extended Liouville Space

The equations of motion, Eq. (5.2), (5.10) and Eq. (5.11), define an extended Liouville space for the dynamics of correlated control and dissipation in terms of [32]

$$\vec{\rho}(t) \equiv \{\rho(t), \mathcal{K}_j, {\mathcal{K}_j}^\dagger; j = 1, 2, 3...\}, \tag{5.12}$$

Therefore, Eq. (5.2), (5.10) and Eq. (5.11) can be combined as

$$\dot{\vec{\rho}}(t) \;=\; \hat{\Lambda}(t) \vec{\rho}(t), \tag{5.13}$$

where $\hat{\Lambda}(t)$ is the generator defined by Eq. (5.2), (5.10) and Eq. (5.11), and can be written as

$$\hat{\Lambda}(\varepsilon(t)) \quad = \quad \hat{\Lambda}_S + \hat{\mathcal{M}}\varepsilon(t). \tag{5.14}$$

where $\hat{\Lambda}_S$ is the field-free component of $\hat{\Lambda}(t)$, and $\hat{\mathcal{M}}$ is the matrix form of the control parameter. The standard solution to Eq. (5.13) is written as

$$\vec{\rho}(t) \quad = \quad \hat{\mathcal{G}}(t,t')\vec{\rho}(t'), \tag{5.15}$$

where the associated propagator can be shown to satisfy

$$\frac{\partial\hat{\mathcal{G}}(t,t')}{\partial t} = \hat{\Lambda}(t)\hat{\mathcal{G}}(t,t'), \tag{5.16}$$

with $\hat{\mathcal{G}}(t,t) = \hat{I}$. The propagator satisfy the following property

$$\hat{\mathcal{G}}(\tau_2,\tau_0) = \hat{\mathcal{G}}(\tau_2,\tau_1)\hat{\mathcal{G}}(\tau_1,\tau_0), \tag{5.17}$$

for ($\tau_2 \geq \tau_1 \geq \tau_0$).

5.3 Optimal Control

In this section, we first introduce the error value we define and the cost function we choose for the optimal control method. Second, we briefly show the algorithm of the optimal control method extended from Krotov's method. Note that in the case without environment influence $\text{Tr}[\rho^2(t)] = 1$ is a dynamical invariance. However, in open quantum systems $\text{Tr}[\rho^2(t)] \leq 1$ is an important decreasing factor that needs to include. For this reason, we choose the error of the control gate satisfy the form

$$\text{Error} \quad = \quad \text{Tr}\{[\mathcal{O} - \mathcal{U}(T)]^2\}/N. \tag{5.18}$$

Here $\mathcal{O}$ stands for the system control target operator. $\mathcal{U}(T)$ is the superoperator for $\rho(T) = \mathcal{U}(T)\rho(0)$ at the target time T, and N is the dimension value of the density matrix $\rho(t)$. To implement the optimal control method for the non-Markovian open quantum system in the extended Liuville space, we first define the fidelity for the extended superoperator $\hat{\mathcal{G}}(T)$ is

$$|\tau| \quad = \quad |\text{Tr}\{\hat{\mathcal{Q}}^\dagger\hat{\mathcal{G}}(T)\}|/\mathcal{N} \tag{5.19}$$

in the form of the extended superoperator as one part of our cost function. Here $\mathcal{Q} = \mathcal{P}_j\mathcal{O}$ is the target operator in the extended Liouville space transformed for the desired operation $\mathcal{Q}$ in the original Liouville space, and $\mathcal{N}$ is the dimension value of the extended matrix

$\mathcal{Q}$. In realistic control problems, energy constraint of the control parameters are included. For the reason, the cost function is of the form

$$J = |\tau| - \int_0^T dt' \lambda(t')(\varepsilon(t') - \varepsilon_0(t'))^2, \tag{5.20}$$

where $\lambda(t)$ is a positive function can be adjusted and chosen empirically, $\varepsilon(t)$ is the control parameter and $\varepsilon_0(t)$ is the standard control value that can be chosen [18, 18]. The reason that we use τ as one part of our cost function instead of $\mathrm{Tr}\{(\hat{\mathcal{Q}} - \hat{\mathcal{G}}(T))^2\}/\mathcal{N}$ is because with the target $\mathcal{Q}$ we still can require the dissipation and the decoherence effects from the auxiliary density matrix $\mathcal{K}_j$ and $\mathcal{K}_j^\dagger$ to approach zero for all the elements not related to $\mathcal{O}$ in $\mathcal{P}_e\mathcal{O}$ are zero [20]. Therefore the required target is enough to implement a quantum gate against the effect from bath. For further understanding, we derive the sufficient and necessary conditions for the different cost function $J' = -\mathrm{Tr}\{(\hat{\mathcal{Q}} - \hat{\mathcal{G}}(T))^2\}/\mathcal{N} - \int_0^T dt' \lambda(t')(\varepsilon(t') - \varepsilon_0(t'))^2$ in Appendix B, and shows that one cannot directly find the sufficient condition for the cost function J'.

Optimal control method used in Refs. [26, 18, 19] allow us to maximize the fidelity $|\tau|$ in Eq. (5.19). To be more specific, consider a time-dependent matrix $\hat{\Lambda}[\varepsilon(t)]$, where $\varepsilon(t)$ is the control parameter. The goal of a quantum optimal control here is to reach a desired target $\hat{\mathcal{O}}$ with high fidelity $|\tau|$ in a certain time T. However, since a direct algorithm to maximize $|\tau|$ was not found, a working alternative is used: optimization of $\mathrm{Re}[\tau]$, or of $\mathrm{Im}[\tau]$, or both. For simplicity, the optimization of the real part $|\tau|$ represented in the cost functional

$$J = \mathrm{Re}[\tau] - \int_0^T dt' \lambda(t')(\varepsilon(t') - \varepsilon_0(t'))^2 \tag{5.21}$$

is used. The optimal algorithm follows the Krotov method [10], and the proof of this cost function satisfy the necessary and sufficient condition for optimality in each iteration is given in Appendix A. The algorithm works as follows:

(i.) An initial guess of $\varepsilon_0(t)$ is chosen for the control parameter.

(ii.) The time-evolution operator $\hat{\mathcal{G}}[\varepsilon_0(t)]$ with the initial condition $\hat{\mathcal{G}}(t = 0) = \hat{I}$ is evolved in time according to the equations of motion, Eq. (5.16), until time T.

(iii.) an auxiliary time-evolution superoperator $\hat{\mathcal{B}}[\varepsilon_k(t)]$, $k = 0$ for the first iteration, with the condition $\hat{\mathcal{B}}(t = T) = \hat{\mathcal{Q}}^\dagger$ is evolved backward in time until $t = 0$ according to the inverse equation of motion

$$\frac{\partial \hat{\mathcal{B}}(t, t')}{\partial t} = \hat{\mathcal{B}}(t, t')\hat{\Lambda}(t) \tag{5.22}$$

(iv.) $\mathcal{B}[\varepsilon_k(t)]$ and $\mathcal{G}[\varepsilon_{k+1}(t)]$ are propagated again forward in time, while the control parameter is updated iteratively with the rule

$$\varepsilon_{k+1}(t) = \varepsilon_k(t) + \frac{1}{2\lambda(t)}\mathrm{Re}[\mathrm{Tr}\{\hat{\mathcal{B}}^{(k)}(t)\frac{\partial\Lambda[\varepsilon(t)]}{\partial\varepsilon(t)}\hat{\mathcal{G}}^{(k+1)}(t)\}], \tag{5.23}$$

and the weight function $\lambda(t)$ constrains the value of the control parameters.

(v.) steps (iii.) and (iv.) are repeated until the required value of the fidelity is obtained. After a sufficient number of iterations, the algorithm converges and reaches asymptotically a maximum τ_{max}. The same procedure can be done even the Hamiltonian contains more than one control parameter.

5.4 Numerical Results and Discussion

we study the one-qubit system coupled to a non-Markovian bosonic bath and subject to a time-dependent external control field $\varepsilon(t)$ [6, 29]. The Hamiltonian in Eq. (5.1) describes a Josephson charge qubit with a control field applied in the gate voltage. Our objective is to realize the state-independent single-qubit Z-gate, i.e.,

$$\mathcal{O} = \begin{pmatrix} 1 & 0 \\ 0 & -1 \end{pmatrix}. \tag{5.24}$$

We use the spectral density of the bath in Eq. (5.6) for different values of the cutoffs and coupling constants. We first show the result for the error of ideal Z-gate and its corresponding optimal pulse. Second, we demonstrate error versus time of the Z-gate under different bath conditions. Finally, the cutoff frequency versus error are discussed and we show that low cutoffs can give high fidelity Z-gate.

5.4.1 Parametrization of the correlation function

As a first step, we need to compare the correlation function of Eq. (5.6) with that obtained numerically in the form of Eq. (5.8). Note that only a few terms in the expansion of Eq. (5.8) are required to model the given correlation function with high accuracy in our cases. The values for Eq. (5.8) were obtained by using MATLAB optimize toolbox with the requirement of the difference $\delta_C(t-t') = C(t-t') - \sum_j C_j(t-t')$ between the actual and the approximated correlation function are chose to be less or equal to 10^{-7}. Fig. 1 shows a comparison of the actual and the approximated correlation function with cutoff ω_c =7.5Ω, α =0.1 and $T = 0.2\Omega$ (here we choose $\Omega = 1$) as the case used in [15], which need more than 48 terms to expand the spectral density function of the ohmic form at the low temperature of $T = 0.2\Omega$. In our situation, we need only three or four terms

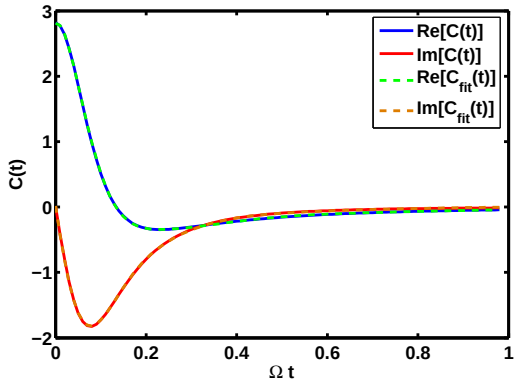

Figure 5.1: (color online). Real and imaginary part of the complex bath correlation function Eq. (5.6) with $\omega_c = 7.5\Omega$, $\alpha = 0.1$, and $T = 0.2\Omega$ and fitting by the exponential functions in Eq. (5.8). Here we named the summary result as $C_{fit}(t-t')$ for convenience.

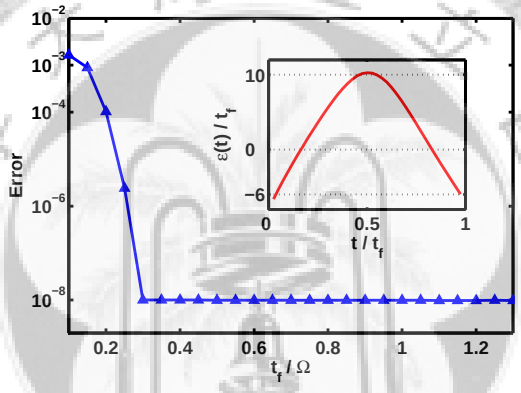

Figure 5.2: (color online). Error versus time for ideal Z-gate and the inset is the optimal control pulse for any $t_f \geq 0.3\Omega$.

to expand the correlation function and the comparison shows a great agreement over the whole range of time in Fig. 1.

5.4.2 Z-gate control

An overview of the ideal Z-gate performance as a function of the duration t_f of the gate is given in Fig. 5.2 with the restriction $\varepsilon(t) \leq 30\Omega$. Excellent Z-gate performance can be achieved for pulse time $t_f \geq 0.3/\Omega$. The corresponding optimal pulse is shown in the inset of Fig. 5.2. Indeed, if one does not require the control field restriction $\varepsilon(t) \leq 30\Omega$, perfect Z-gate can be achieved for any finite period of time t_f. For the reason, this optimal control pulse gives an advanced choice of the control filed pulse to implement a Z-gate as compared with the Z-gate in [20] which requires the gate operation time $\geq \pi/\Omega$. Besides, the inset of Fig. 5.2 also shows the strategy of the optimal control pulse. As the $\Omega\sigma_x$ term is always on, the optimal control first gives a negative magnitude corresponding

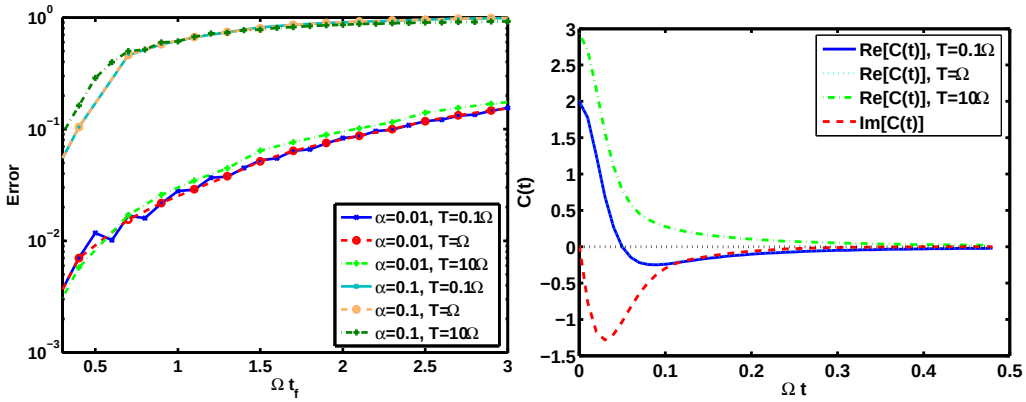

Figure 5.3: The left panel is the error of the Z-gate versus time with $\omega_c = 20\Omega$ for different values of α and T. The stopping criteria of the error threshold is set to 10^{-5} or when the number of iterations exceeds 3000 times. The right panel is the corresponding correlation function for $\alpha = 0.01$

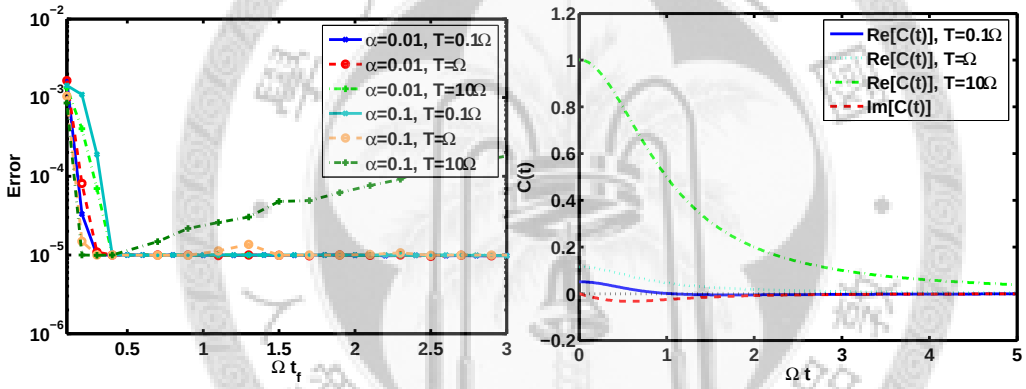

Figure 5.4: The left panel is the error of the Z-gate versus time with $\omega_c = \Omega$ for different values of α and T. The right panel is the corresponding correlation function for $\alpha = 0.1$

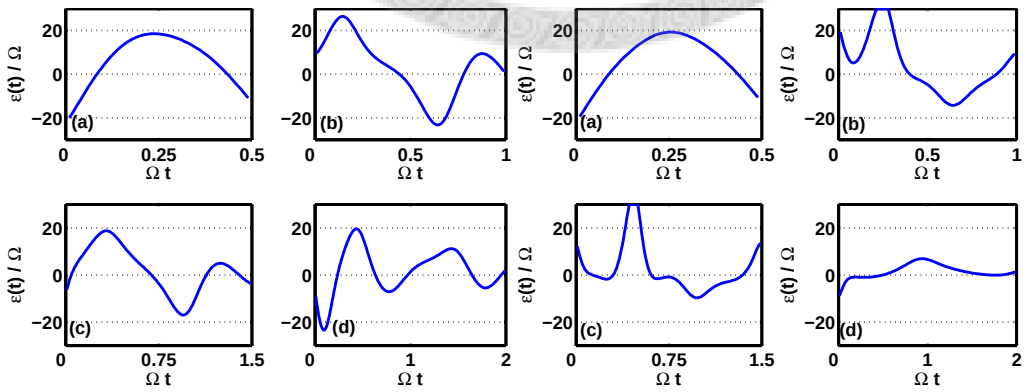

Figure 5.5: (color online). Left four panels are the optimal pulses for $\alpha = 0.01$, $\omega_c = \Omega$ in different values of time t_f= (a)0.5/Ω, (b)1/Ω, (c)1.5/Ω (d)2/Ω. Right four panels are the optimal pulses for $\alpha = 0.01$, $\omega_c = 20\Omega$ and $T = \Omega$ in different values oft_f = (a)0.5/Ω, (b)1/Ω, (c)1.5/Ω (d)2/Ω.

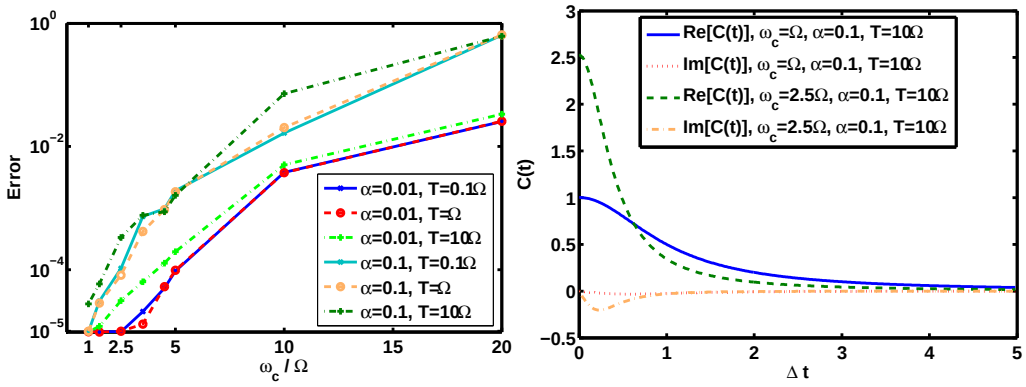

Figure 5.6: (color online). The left panel is the error of the Z-gate versus cutoff ω_c with $t_f = 1/\Omega$. . The right is corresponding correlation function of the conditions: $\alpha = 0.1$, $T = 10\Omega$, $\omega_c = \Omega$ and $\omega_c = 2.5\Omega$.

to an inverse rotation of σ_z, which can reduce the contribution by $\Omega\sigma_x$ from the direct rotation of σ_z. Finally the same process is performed for the same reason. This strategy of the optimal control pulse with symmetric pulse shape also gives the minimum energy consumption. The optimal control pulse can be approximately written as the form: $\varepsilon(t) = (16/t_f)\sin(\pi t/t_f) - (6/t_f)$.

An important question to be addressed is whether the different cutoff ω_c of the non-Markovian environment influence the error of a Z-gate. In Fig. 5.3, we show that for the case of $\omega_c = 20\Omega$, the error will increase when operation time become longer. The error for the case of smaller $\alpha = 0.01$ is about 10^{-3} at the beginning and quickly increase to 10^{-1} in very short time. The reason is that when $\omega_c = 20\Omega$, the environment is becomes very close to a Markovian environment, and therefore the memory effect is extremely weak. The decay rate approaches to a constant values in a very short time and thus is almost unchangeable by the optimal control. In this case, the environment contribution cannot be revised. We also find that the value of the coupling strength plays the most important role in determining the amount of the error in this case. This can be understood by the correlation function in Fig. 5.3. The correlation function at time $t = 0$ for the high temperature ($T = 10\Omega$) is only bigger than the low temperature ($T = \Omega$) by a factor of 1.5. However, the coupling strength is different by a factor of 10. Therefore, the main factor of the environment influence for the case $\omega_c = 20\Omega$ is from the value of the coupling strength.

On the other hand, for the case of $\omega_c = \Omega$, the result is totally different. In Fig. 5.4 we shows that it is possible to reduce the error of building a Z-gate to below 10^{-5} even for a long time period. This can be explained from the memory effect of non-Markovian environment. Since the correlation function in Fig. 5.4 shows a long-smooth amplitude and approaches 0 in a time scale of $t = 1/\Omega$, this allows the optimal control field to

counteract the contribution from the environment during this longer bath correlation time. However, It is not possible to reduce all the effects from environment to build a Z-gate for all cases considered in Fig. 5.4. As a result, even though the error can be reduced to below 10^{-5} at the beginning, the influence of the environment still will increase the error as time become longer. Besides, for the case of $\omega_c = \Omega$, the temperature plays an important role similar to the coupling strength. The amplitude ratio of the bath correlation function between the temperature $T = 10\Omega$ case and $T = \Omega$ case is about 10 which is fundamentally different from the situation of $\omega_c = 20\Omega$, shows in Fig. 5.3.

In Fig. 5.5 we show the optimal pulses in different times under the condition $\alpha = 0.01$, $T = \Omega$. The cutoff frequency is $\omega_c = \Omega$ for the left four panels and is $\omega_c = 20\Omega$ for the right four panels. For the case of a short gate operation time of $t_f = 1/\Omega$, we find that the optimal pulse shapes are approximately similar to the ideal case shown in the inset of Fig. 5.2. However, when the gate operation time become longer, the optimal pulse shapes show significant difference from the short gate operation time case and different cutoffs also show different pulse shapes. The optimal pulses for operation of times $t = 1/\Omega$ and $1.5/\Omega$ approximately follow the similar strategy for both the cutoff cases but seem to take different optimal strategy for operation time $t_f = 2/\Omega$. We further investigate the dependence of the gate error on the cutoffs of the open qubit system. Fig. 5.6 shows the gate error versus cutoff ω_c at time $t = 1/\Omega$ for different values of the coupling strength α and temperature T. One can see that the gate error depends strongly on the bath cutoff frequence. The error increases as the cutoff becomes bigger. For the weak coupling and low temperature cases ($\alpha = 0.01$, $T \leq \Omega$), it is possible to reduce the error to below 10^{-5} for the cutoff between $\Omega \geq \omega_c \leq 2.5\Omega$. This explains the robustness of optimized Z-gate against non-Markovian environment processes. However, in the case $\alpha = 0.01$, $T = 10\Omega$, as the cutoff increase to $\omega_c \gg 5$, the gate error becomes large than 10^{-5}. This phenomenon can be explained from the rapid change of the bath correlation function in the right panel of Fig. 5.6. We find that the amplitude of correlation function at $t = 0$ for $\omega_c = 2.5\Omega$ case is much bigger than that of $\omega_c = \Omega$ case, and the bath correlation time for $\omega_c = 2.5$ case is relatively smaller than $\omega_c = \Omega$ case. Therefore, the gate error is increases rapidly as the cutoff increases under the conditions. The similar behaviours processes have been investigated and observed for the X-gate case.

5.5 Conclusion

In summary, an optimal control method is constructed for a time-nonlocal or time-convolution non-Markovian open quantum system with a dissipator in which the control field and the bath dissipation are correlated. The optimal control method is developed based on a novel

quantum dissipation formulation that transforms the nonlocal-in-time master equation to a set of coupled linear local-in-time equations of motion of the original density matrix and auxiliary density matrices in an extended Liouville space. State-independent superoperator formulation is considered to implement quantum gate operations. As an illustration, the optimal control method is applied to find the control field sequence for a single-qubit Z-gate in a superconducting charge qubit model embedded in a non-Markovian bosonic bath. It is possible to achieve high-fidelity Z-gate with error less than 10^{-4} for the non-Markovian open qubit system. The control-dissipation correlation and the memory effect of the bath are crucial in achieving the high-fidelity gates.

Appendix A: Iterative solution scheme based on necessary and sufficient conditions for optimality

Using the cost function mentioned in Eq. (5.20)

$$J = Re[\mathtt{Tr}\{\mathcal{Q}^{\dagger}\mathcal{G}(T)\}]/\mathcal{N} - \int_0^T dt\lambda(t)|\varepsilon(t) - \bar{\varepsilon}(t)|^2, \tag{5.25}$$

in the following discussion we will prove that the iteration algorithm for the cost function J exhibits monotonically convergence. For convenience we set the dimension number $\mathcal{N} = 1$. First, following the Krotov's method [26, 10], we partition J in the following suggestive form

$$\bar{J} = G(T) + \int_0^T dt R(t). \tag{5.26}$$

Here $G(T)$ depends only on the terminal time T and is defined as the form

$$G(T) \equiv \mathrm{Re}\left[\mathtt{Tr}\{\mathcal{Q}^{\dagger}\mathcal{G}(T)\} - \mathtt{Tr}\{\mathcal{B}(\mathtt{t})\mathcal{G}(\mathtt{t})\}\Big|_0^{\mathtt{T}}\right], \tag{5.27}$$

where $\mathcal{B}(t)$ is an arbitrary continuously differentiable propagator which can be considered as the Lagrange multiplier function constraining the system to obey the equation of motion. $R(t)$ is related to a time integral part and of is the form

$$\begin{aligned} R(t) \equiv\ & \mathrm{Re}\left[\mathtt{Tr}\{\mathcal{B}(\mathtt{t})(\hat{\Lambda}_{\mathtt{s}} + \hat{\mathcal{M}}\varepsilon(\mathtt{t}))\mathcal{G}(\mathtt{t}) + \frac{\partial\mathcal{B}(\mathtt{t})}{\partial\mathtt{t}}\mathcal{G}(\mathtt{t})\}\right] \\ & -\lambda(t)|\varepsilon(t) - \bar{\varepsilon}(t)|^2. \end{aligned} \tag{5.28}$$

For simplicity, here we choose only one control parameter for the generator $\hat{\Lambda}(t)$, and for multi-parameters case the result can be derived following the same process. To maximize $\bar{J}$ one proceeds to maximize G and R independently. Note that if R is maximized at each

time t the integral of R will be maximized. Second, to prove that $\bar{J}$ converge in every iteration, it is straightforward to show that

$$\bar{J}^{(k+1)} - \bar{J}^{(k)} = \Delta_1 + \Delta_2 + \Delta_3 \geq 0 \tag{5.29}$$

where

$$\begin{aligned} \Delta_1 &\equiv G(\mathcal{G}^{(k+1)}(T)) - G(\mathcal{G}^{(k)}(T)) \\ &= \mathrm{Re}[\mathtt{Tr}\{(\mathcal{Q}^\dagger - \mathcal{B}(\mathtt{T}))\Delta\mathcal{G}(\mathtt{T})\}], \end{aligned} \tag{5.30}$$

$$\begin{aligned} \Delta_2 &\equiv \int_0^T dt[R(t, \mathcal{G}^{(k+1)}(t), \varepsilon^{(k+1)}(t)) - R(t, \mathcal{G}^{(k+1)}(t), \varepsilon^{(k)}(t))] \\ &= Re\left[\int_0^T dt\mathtt{Tr}\{\mathcal{B}(\mathtt{t})(\hat{\mathcal{M}}\Delta\varepsilon(\mathtt{t}))\mathcal{U}^{(\mathtt{k+1})}(\mathtt{t})\}\right] \\ &\quad - \int_0^T dt 2\lambda(t)(\varepsilon^{(k+1)}(t) - \bar{\varepsilon}(t))\Delta\varepsilon(t) + \lambda(t)\Delta\varepsilon^2(t), \end{aligned} \tag{5.31}$$

$$\begin{aligned} \Delta_3 &\equiv \int_0^T dt[R(t, \mathcal{G}^{(k+1)}(t), \varepsilon^{(k)}(t)) - R(t, \mathcal{G}^{(k)}(t), \varepsilon^{(k)}(t))] \\ &= Re\left[\int_0^T dt\mathtt{Tr}\{(\mathcal{B}(\mathtt{t})(\hat{\Lambda}_S + \hat{\mathcal{M}}\varepsilon^k(t))\Delta\mathcal{G}(t)\}\right. \\ &\quad \left. - \int_0^T dt\mathtt{Tr}\{\frac{\partial\mathcal{B}(\mathtt{t})}{\partial\mathtt{t}})\Delta\mathcal{G}(\mathtt{t})\}\right]. \end{aligned} \tag{5.32}$$

Here $\Delta\varepsilon = \varepsilon^{(k+1)}(t) - \varepsilon^{(k)}(t)$ and $\Delta\mathcal{G}(t) = \mathcal{G}^{(k+1)}(t) - \mathcal{G}^{(k)}(t)$, and in deriving these expressions we also have choose $\mathcal{B}(t) \equiv \mathcal{B}^{(k)}(t)$ in the expression for $\bar{J}^{(k+1)}$ as well as in that for $\bar{J}^{(k)}$. Third, we can acquire the equation of motion and initial state of $\mathcal{B}(t)$ by making the choice

$$\mathcal{B}(T) = \mathcal{Q}^\dagger, \tag{5.33}$$

$$\frac{\partial\mathcal{B}(t)}{\partial t} = \mathcal{B}(t)(\hat{\Lambda}_S + \hat{\mathcal{M}}\varepsilon^k(t)), \tag{5.34}$$

Therefore we obtain the result

$$\Delta_1 = 0, \tag{5.35}$$

$$\Delta_3 = 0. \tag{5.36}$$

Finally, the control parameter $\varepsilon^{(k+1)}(t)$ can be decided by choosing

$$\varepsilon^{(k+1)}(t) = \bar{\varepsilon}(t) + \frac{1}{2\lambda(t)} Re\left[\mathtt{Tr}\{\mathcal{B}(\mathtt{t})\hat{\mathcal{M}}\mathcal{G}^{(\mathtt{k+1})}(\mathtt{t})\}\right], \tag{5.37}$$

This expression also suggests that

$$\Delta_2 \;=\; \lambda(t)(\Delta\varepsilon)^2 \geq 0. \tag{5.38}$$

Here $\lambda(t)$ is a positive function can be decided empirically. The results here prove that the iteration algorithm for cost function J exhibits monotonically convergence with the proper choice of the equation of motion and initial condition for $\mathcal{B}(t)$, and the optimal control parameter at the next time step is also decided. Note that $\bar{\varepsilon}(t)$ in the k+1 iteration can be substituted by the optimal control parameter $\varepsilon^{(k)}(t)$ acquired in the k iteration. Similarly, the result of the multi-parameters cases is of the form

$$\varepsilon^i_{k+1}(t) = \bar{\varepsilon}^i(t) + \frac{1}{2\lambda(t)} Re[\mathrm{Tr}\{\hat{\mathcal{B}}^{(k)}(t)\hat{\mathcal{M}}^i\hat{\mathcal{G}}^{(k+1)}(t)\}], \tag{5.39}$$

here i is the notation for multi-parameters and $\hat{\mathcal{M}}^i$ is the matrix product with $\varepsilon^i(t)$. For linear cases, $\hat{\mathcal{M}}^i$ can be written as $\partial\Lambda[\vec{\bar{\varepsilon}}(t)]/\partial\varepsilon^i(t)$ with $\hat{\Lambda}(\vec{\bar{\varepsilon}}(t)) = \hat{\Lambda}_S + \sum_i \hat{\mathcal{M}}^i\varepsilon^i(t)$.

Appendix B: Necessary and sufficient conditions for cost function J'

Since we already show the monotonically convergence condition in Appendix A, now we will briefly calculate the sufficient and necessary conditions for

$$J' \;=\; -\mathrm{Tr}\{(\hat{\mathcal{Q}} - \hat{\mathcal{G}}(T))^2\}/\mathcal{N} - \int_0^T dt\lambda(t)|\varepsilon(t) - \bar{\varepsilon}(t)|^2. \tag{5.40}$$

For simplicity, we also set the dimension number $\mathcal{N} = 1$. First, by following the Krotov's method, we partition J' into

$$\bar{J}' \;=\; G'(T) + \int_0^T dtR(t), \tag{5.41}$$

where One can easily find that $R(t)$ satisfies the same form derive in Appendix A. Therefore, equation of motion for backward propagator $\mathcal{B}(t)$ and the control field $\varepsilon^{(k+1)}(t)$ for the next iteration are also the same as the results derived in Appendix A. The only difference is the expression of $G'(T)$ which now can be written as

$$G'(T) \;\equiv\; -\mathrm{Tr}\{(\hat{\mathcal{Q}} - \hat{\mathcal{G}}(T))^2\} - Re\left[\mathtt{Tr}\{\mathcal{B}(\mathtt{t})\mathcal{G}(\mathtt{t})\}\Big|_0^{\mathtt{T}}\right]. \tag{5.42}$$

To inspect the sufficient and necessary conditions of $G'(T)$, we check that

$$\begin{aligned}\Delta'_1 \;&\equiv\; G'(\mathcal{G}^{(k+1)}(T)) - G'(\mathcal{G}^{(k)}(T)) \\ &=\; Re[\mathtt{Tr}\{((\mathcal{Q}^\dagger - \mathcal{G}^\dagger(\mathtt{T})) - \mathcal{B}(\mathtt{T}))\Delta\mathcal{G}(\mathtt{T})\}] - |\Delta\mathcal{G}(\mathtt{T})|^2,\end{aligned} \tag{5.43}$$

where $\Delta\mathcal{G} = \mathcal{G}^{(k+1)} - \mathcal{G}^{(k)}$. Since there is no direct way to choose $\mathcal{B}(T)$ satisfy the sufficient condition, we can use $\frac{\partial G'(T)}{\partial \mathcal{G}(T)} = 0$ to find the necessary condition that $\mathcal{B}(T)$ satisfies. The result of the derivative is

$$\mathcal{B}(T) \;=\; 2(\mathcal{Q}^{\dagger} - \mathcal{G}^{\dagger}(T)). \tag{5.44}$$

We then obtain the result

$$\Delta' = -|\Delta\mathcal{G}(T)|^2 \leq 0. \tag{5.45}$$

We therefore show that the cost function Eq. (5.40) satisfies only the necessary condition and has a second order contribution from Δ' which will influence the convergence and will require the energy constraint $\lambda(t)$ must satisfy the condition

$$\lambda(t)(\Delta\varepsilon(t))^2 \;\geq\; |\Delta\mathcal{G}(T)|^2. \tag{5.46}$$

This restriction may confine the range that can be used for $\lambda(t)$ and give a worse result for quantum gate operations.

Chapter 6

Conclusion

In this thesis we present a general optimal control theory for Non-Markovian open quantum systems based on the superoperator formalism. Therefore we do not require the knowledge of the initial states of density matrix. We treats the effect of the bath correlation function of the non-Markovian dissipation as auxiliary density matrices coupled to qubits in an extended Liouville space. The extended propagator is formulated for both the forward propagation of the extended density operator and the backward propagation of the extended target operator; both depend on the control field parameters. This approach is used to study a quantum gate for a superconducting qubit system within a spin-boson model. The time-convolution master equation was computed within the second-order perturbation theory in the spin-boson interaction leading to a control-dissipation correlated dissipator. Note, however, that the coupling between the system and external control field is treated nonpertubatively.

With such a general formalism we presented optimal control pulses to implement a Z-gate for different values of environment parameters, such as the temperature, the cutoff frequency, and the coupling strength. For the ohmic bath spectral density we chose for the investigation, we find that the gate fidelity or gate error depends strongly on the cutoff frequency. The gate error increases as the cutoff frequency decreases. As expected, when the system-bath coupling strength and the bath temperature increase, the gate error also increases. It is possible to achieve a high-fidelity Z-gate with gate error smaller than 10^{-5} in this non-Markovian spin-boson model.

In the past, the Markovian approximation is widely used and assumed to be valid in most of the cases, while in some systems the Markovian approximation may not valid any more. Here we find in non-Markovian open quantum system the control-dissipation correlation can be optimized to countered the environment effect when the bath memory effect time is large and coupling strength is relatively weak. On the other hand, for the Markovian case, the optimal control cannot effectively reduce decay or dephasing rate as

they approach to a constant value in a rather small time scale (assume to be instaneous in the Markovian limit). It can only reduce the bath effect on the system dynamics under the constant dissipation. Therefore, we can conclude that the control-dissipative correlation and memory effect really play an important role on changing the contribution of environment to the system.

The optimal control method presented is extremely efficient to deal with the time-nonlocal non-Markovian equation of motion, and thus open the way to investigating two-qubits and many-qubits problems in time-dependent dissipative environment. However, by extending to more qubits problems, the dimension of the extended density matrix will grow up rapidly, and the numerical demonstration would take more time to compute. Our future objective is to extend this work to the implementation of two-qubit quantum gate operations.

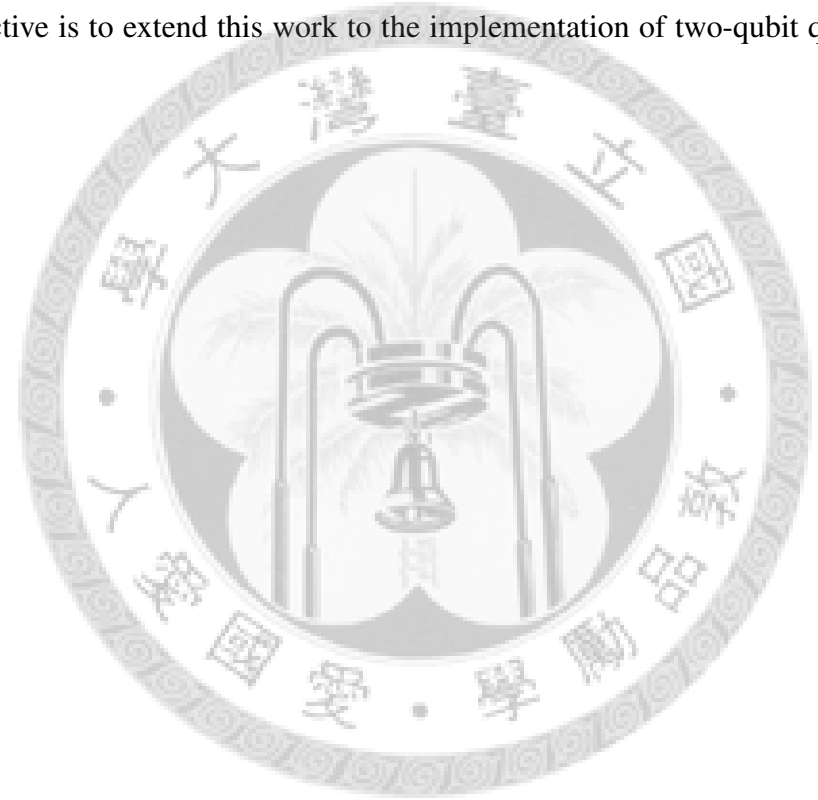

Bibliography

[1] J. T. Barreiro, M. Muller, P. Schindler, D. Nigg, T. Monz, M. Chwalla, M. Hennrich, C. F. Roos, P. Zoller, and R. Blatt. An open-system quantum simulator with trapped ions. *Nature*, 470(7335):486–491, Feb. 2011.

[2] H. J. Carmichael. *Statistical Methods in Quantum Optics 1*. 1999.

[3] J. Clarke and F. K. Wilhelm. Superconducting quantum bits. *Nature*, 453(7198):1031–1042, June 2008.

[4] W. Cui, Z. R. Xi, and Y. Pan. Optimal decoherence control in non-markovian open dissipative quantum systems. *Phys. Rev. A*, 77(3):032117, Mar 2008.

[5] F. P. Heinz-Peter Breuer. *The Theory of Open Quantum Systems*. OXFORD, 2006.

[6] H. Jirari. Optimal control approach to dynamical suppression of decoherence of a qubit. *EPL (Europhysics Letters)*, 87(4):40003, 2009.

[7] H. Jirari and W. Pötz. Quantum optimal control theory and dynamic coupling in the spin-boson model. *Phys. Rev. A*, 74(2):022306, Aug 2006.

[8] H. Jirari and W. Pötz. Optimal control of dissipation for the example of the spin-boson model. *EPL (Europhysics Letters)*, 77(5):50005, 2007.

[9] C. Kittel. *Introduction to Solid State Physics, 8 ed.* 2004.

[10] V. F. Krotov. *Global methods in optimal control theory*. Marcel Dekker, Inc, 1996.

[11] Li, G.-Q. and Kleinekathöfer, U. Optimal control of shot noise and fano factor by external fields. *Eur. Phys. J. B*, 76(2):309–319, 2010.

[12] J. M. M. M. H. Devoret, A. Wallraff. Superconducting qubits: A short review. *arxiv:cond-mat*, 2005.

[13] Y. Makhlin, G. Schön, and A. Shnirman. Quantum-state engineering with josephson-junction devices. *Rev. Mod. Phys.*, 73(2):357–400, May 2001.

[14] I. I. Maximov, Z. Tošner, and N. C. Nielsen. Optimal control design of nmr and dynamic nuclear polarization experiments using monotonically convergent algorithms. *The Journal of Chemical Physics*, 128(18):184505, 2008.

[15] C. Meier and D. J. Tannor. Non-markovian evolution of the density operator in the presence of strong laser fields. *The Journal of Chemical Physics*, 111(8):3365–3376, 1999.

[16] S. Montangero, T. Calarco, and R. Fazio. Robust optimal quantum gates for josephson charge qubits. *Phys. Rev. Lett.*, 99(17):170501, Oct 2007.

[17] C. J. Myatt, B. E. King, Q. A. Turchette, C. A. Sackett, D. Kielpinski, W. M. Itano, C. Monroe, and D. J. Wineland. Decoherence of quantum superpositions through coupling to engineered reservoirs. *Nature*, 403(6767):269–273, Jan. 2000.

[18] J. P. Palao and R. Kosloff. Quantum computing by an optimal control algorithm for unitary transformations. *Phys. Rev. Lett.*, 89(18):188301, Oct 2002.

[19] J. P. Palao and R. Kosloff. Optimal control theory for unitary transformations. *Phys. Rev. A*, 68(6):062308, Dec 2003.

[20] P. Rebentrost, I. Serban, T. Schulte-Herbrüggen, and F. K. Wilhelm. Optimal control of a qubit coupled to a non-markovian environment. *Phys. Rev. Lett.*, 102(9):090401, Mar 2009.

[21] R. Roloff and W. Pötz. Time-optimal performance of josephson charge qubits: A process tomography approach. *Phys. Rev. B*, 79(22):224516, Jun 2009.

[22] R. Roloff, M. Wenin, and W. Potz. Optimal control for open quantum systems: Qubits and quantum gates. *Journal of Computational and Theoretical Nanoscience*, 6:1837–1863(27), August 2009.

[23] S. Safaei, S. Montangero, F. Taddei, and R. Fazio. Optimized single-qubit gates for josephson phase qubits. *Phys. Rev. B*, 79(6):064524, Feb 2009.

[24] F. Shuang and H. Rabitz. Cooperating or fighting with decoherence in the optimal control of quantum dynamics. *The Journal of Chemical Physics*, 124(15):154105, 2006.

[25] A. Spörl, T. Schulte-Herbrüggen, S. J. Glaser, V. Bergholm, M. J. Storcz, J. Ferber, and F. K. Wilhelm. Optimal control of coupled josephson qubits. *Phys. Rev. A*, 75(1):012302, Jan 2007.

[26] D. J. Tannor, V. Kazakov, and V. Orlov. Control of Photochemical Branching: Novel Procedures for Finding Optimal Pulses and Global Upper Bounds. In J. Broeckhove & L. Lathouwers, editor, *NATO ASIB Proc. 299: Time-Dependent Quantum Molecular Dynamics*, pages 347–360, 1992.

[27] M. Tinkham. *Introdunction to Superconductivity: Second Edition*. 2004.

[28] J. C. Tremblay and P. Saalfrank. Guided locally optimal control of quantum dynamics in dissipative environments. *Phys. Rev. A*, 78(6):063408, Dec 2008.

[29] M. Wenin and W. Pötz. Minimization of environment-induced decoherence in quantum subsystems and application to solid-state-based quantum gates. *Phys. Rev. B*, 78(16):165118, Oct 2008.

[30] M. Wenin, R. Roloff, and W. Pötz. Robust control of josephson charge qubits. *Journal of Applied Physics*, 105(8):084504, 2009.

[31] R. Xu and Y. Yan. Theory of open quantum systems. *The Journal of Chemical Physics*, 116(21):9196–9206, 2002.

[32] R. Xu, Y. Yan, Y. Ohtsuki, Y. Fujimura, and H. Rabitz. Optimal control of quantum non-markovian dissipation: Reduced liouville-space theory. *The Journal of Chemical Physics*, 120(14):6600–6608, 2004.

[33] T. Yamamoto, Y. A. Pashkin, O. Astafiev, Y. Nakamura, and J. S. Tsai. Demonstration of conditional gate operation using superconducting charge qubits. *Nature*, 425(6961):941–944, Oct. 2003.

[34] J. Q. You and F. Nori. Superconducting circuits and quantum information. *Physics Today*, 58(11):42–47, 2005.